ELECTRON TRANSFER PROCESSES IN DISORDERED MEDIA*

EWA GUDOWSKA-NOWAK

Department of Statistical Physics
Institute of Physics, Jagellonian University
Reymonta 4, 30-059 Kraków, Poland

(Received August 18, 1995)

The paper reviews a broad range.of approaches to the chemical dynamics in condensed phase systems. We analyze the problem of thermal electron transfer in disordered media (proteins) and discuss the interplay of quantum tunnelling effects, electronic nonadiabaticity, friction and conformational changes on kinetic rate of the process.

PACS numbers: 05.20. Dd, 05.40. +j, 82.20. Fd, 87.15. Rn

CONTENTS

* This paper is presented as the qualifying thesis for the habilitation at the Jagellonian University.

1. Introduction

1.1. Problems of chemical kinetics in disordered media

There has been a considerable recent growth of research activities concerned with relaxation and transport in condensed-matter systems, such as amorphous and porous materials, glass-forming liquids, polymer melts, biological membranes and proteins [1, 2]. The approach to equilibrium in such systems is generally characterized by time-dependent linear responses such as dispersive transport and nonexponential correlation functions, and by anomalous dependence of the transport or relaxation time on a number of experimental variables. A common belief is that these features are due both to the effects of dynamical interactions between the relevant degrees of freedom and to effects of the static disorder of the material.

The understanding of transport properties in condensed phases is of fundamental importance in furthering our knowledge of structure and functionality of biological systems. The key to carrying out the description of the kinetic rate in complex system is to identify the major energy scales in the problem. Existence of large energy gaps leads quantum mechanically to the separation of "slow" and "fast" variables being the crux of the Born–Oppenheimer approximation. This allows to solve the electronic problem at fixed vibrational coordinates which are treated as classical coordinates subject to thermodynamic fluctuations. In this context, the theory of kinetic rate incorporates quantum mechanical estimates of Born–Oppenheimer potential energy surfaces and dissipative motion of nuclear coordinates described conveniently in terms of stochastic dynamics. The interplay of these two factors is essential for understanding the degree of temperature-dependent kinetics.

Chemical reactions govern all aspects of biological processes, from enzyme catalysis to the transfer of charge, matter and information. Most of the knowledge of reaction dynamics, however, has been deduced from the

studies of two-body interactions of small molecules in the gas phase [3]. In contrast to this simple system, biomolecules provide a complex but highly organized environment that can affect the course of the reaction.

The free energy surface of the complex chemical reaction going on in a disordered medium is "rough" [4, 5, 6] (*i.e.* it has many saddle points and local minima representing *e.g.* various conformational metastable states of the medium). Distribution of the roughness of such a stochastic energy landscape determines relaxation dynamics [7, 5, 8] and may be responsible for dynamic, temperature dependent phase change in the medium [1]. The principal goal in understanding complex dynamics is thus to explore kinetics in disordered systems within two distinct categories of disorder:

— static disorder (fluctuations of metastable states follow a much shorter time scale than the kinetic process of interest)

— dynamic disorder (time evolution of fluctuations mediating the kinetics occurs at the similar or longer time scale than the kinetic process of interest).

One of the most intriguing biophysical problems is theoretical interpretation of the mechanisms of conversion and storage of energy involved in oxido-reduction reactions in which an electron is transferred along a chain of redox centers embedded in a protein medium [9, 10, 11, 5, 12]. The standard picture of photoinduced electron transfer (ET) involves the coupling of two electronically excited states, a neutral state and a charge transfer state, to a single nuclear degree of freedom, *i.e.*, the reaction coordinate. This coordinate may be collective in nature, such as solvent polarization, or may correspond to a specific vibrational motion of a protein or lattice. The electronic interaction gives rise to a splitting of the energy levels in the region where the neutral and the charge transfer potential energy surfaces intersect. The majority of nuclear degrees of freedom constitute a thermal bath. The coupling between the system and bath degrees of freedom introduces dissipation into the system. The transfer of an electron is usually thought to be triggered by a fluctuation of the dielectric polarization in the surrounding medium. The dynamics of such fluctuations is determined by the finite response time, which under certain conditions, can become the rate determining factor of the reaction.

The aim of this survey is to present basic ideas of modern kinetic rate theory devoted to studies of relaxation and transport properties in natural systems. The presentation is based on a series of our papers published elsewhere, [13–19].

Chapters 1 and 2 review main concepts of the electron transfer reactions in the context of natural systems. In Section 2.2 we discuss shortly limitation of use of a standard approach to the kinetic rate problem based on use of the "generalized" Smoluchowski diffusion equation (a critical overview of

the method has been published by the author separately in [17]). Chapter 3 is a glance over various derivation of formula for the kinetic rate constant in a stochastic medium with author's contribution presented in Section 3.2. Chapter 4 is devoted to biophysical applications of ET theory and includes main results of the thesis. In particular, it is shown, that complexity of a potential surface describing the states before and after the electron transfer leads to the overall enhancement of the rate (Section 4.2). Our discussion of electron-transfer processes refers to analysis of stochastic effects entering nuclear and electronic factors controlling the rate (Section 4.3). To study the effect of heterogeneous media on electronic tunneling in proteins, we introduce the concept of a "diffusive pathway"(Section 4.4) and classify electron transfer probabilities limited by stochastic motions of interchromophore spacers. As a direct application of the formalism, we discuss nonexponential relaxation dynamics and electron transfer rates in photosynthetic reaction centers (Sections 4.3 and 4.4 and 4.5).

1.2. General concepts of ET reactions

Since the pioneering work of Marcus [20] conventional ET theory is based on the Condon approximation which assumes that the electronic coupling depends only on the donor-acceptor distance but not on the nuclear coordinates [21, 22, 23]. As a result, the coupling term in the golden rule expression of the electron transfer rate can be separated from the Franck–Condon factor which contains only overlap integrals of nuclear coordinates. Similarly, in an alternative ET description in the framework of spin-boson model [24], one assumes that a coupling matrix element is constant in time and depends only on the initial and final electronic states. The Condon approximation is ideal for intramolecular ET in system with a rigid spacer or for intermolecular electron transfer in systems with the donor and acceptor firmly held by binding to rigid matrices. The validity of this approximation breaks down when modelling ET with a floppy spacer or for intermolecular electron transfer in solutions.

One of the crucial issues in biological ET is the determination of the role of spatially intermediate amino acid residues in controlling or directing the electronic tunnelling interactions between redox sites. Traditional quantum mechanical methods which can be valuable in determining physico-chemical properties of single amino acids and prosthetic groups are usually intractable for problems involving whole proteins. Among various methods used in the field there are semi-empirical one electron theories advanced by Beratan and Hopfield [10] and by Larsson [25, 26] which discuss the concept of through-bond interactions in bridged donor-acceptor systems. An alternative approach has been proposed by Wolynes and Kuki [9, 27, 28] who examined

tools based on real space quantum propagators[1]. The path integral theory developed by these authors has been applied to study intramolecular ET in a ruthenium-modified myoglobin, so far the only successful example of the method that has been implemented in proteins at the one-electron Hamiltonian level[2]. In this formalism, the analysis of tunneling in a multistable potential relies on a classification of the paths that contribute to the path integral

$$\langle 1|e^{-\beta H}|2\rangle = \int dx_i \psi_1(x_i) \int dx_f \psi_2(x_f) \int_{x_i}^{x_f} \mathcal{D}x(\beta) \exp\left\{-\int_0^\beta H(x(\beta'))d\beta'\right\}, \tag{1.1}$$

where H is the Hamiltonian of the system, β is the inverse thermal energy, x_i and x_f are coordinates of initial and final "states", respectively, and the $\mathcal{D}$ symbol indicates path integration. A typical path which contributes to the above expression is the one which stays in the donor potential well for a relatively long time before rapidly making a transit to the acceptor well, where it resides again for a relatively long period of time. Such a rapid transit is called a "kink". Other paths contributing to the path sum will have a larger but odd number of such kinks. The kinks, typically well separated in time, can be considered noninteracting. The contribution of paths with N kinks to the path sum is then

$$\frac{1}{N!} e^{-N\beta F_k} e^{-\beta E_0}, \tag{1.2}$$

where F_k is the free energy of introducing a kink[3] and factor $N!$ comes from indistinguishability of the kinks. The amplitude for a transition from "state 1" to "state 2" can be represented as the sum

$$e^{-\beta E_0} \sum_{\text{odd}} \frac{1}{N!} e^{-N\beta F_k} = e^{-\beta E_0} \sinh(e^{-\beta F_k}), \tag{1.3}$$

and should be compared with the quantum mechanics result which for the system of two nearly degenerate states with energies $E_0 \pm \Delta$ yields the same amplitude in the form of

$$e^{-\beta E_0} \sinh(\beta \Delta). \tag{1.4}$$

---

[1] This approach avoids strong dependence on the tails of basis functions used in traditional basis set quantum methods, *cf.* [9, 21].

[2] In recent reviews, Kuki *et al.* [9] present a generalization of the method to multi-electron Hamiltonians.

[3] F_k is a difference between the free energy of a one-kink path and that of a path confined to one well E_0.

Thus the tunneling amplitude Δ is exponentially related to the free energy of introducing a kink:

$$\Delta = \beta^{-1} e^{-\beta F_k} . \tag{1.5}$$

A tunneling matrix element Δ gives the probability amplitude for transitions between potential energy surfaces characteristic for electronic configurations before and after the ET transfer estimated at fixed nuclear configurations. If Δ sufficiently small, second-order perturbation theory gives a "golden rule" expression for the rate of transition between the two electronic states as a thermal average of the rate between two particular nuclear-motion eigenstates on each of two potential energy surfaces:

$$k_{\mathrm{ET}} = \frac{2\pi}{\hbar} \langle |H_{if}|^2 \rho_f(E_i) \rangle , \tag{1.6}$$

where H_{if} is the perturbation matrix element between the initial and final vibronic states and $\rho_f(E_i)$ is the density of final states at the initial energy.

In semiclassical theories of tunneling, an extremal one kink path is found. The free energy F_k is then the action associated with an extremal path plus contributions from small amplitude oscillations around the path which are treated harmonically. The extremal path can be easily determined in a classical flat potential where the action of a straight line path is proportional to its length giving rise to Δ proportional to e^{-r}.

For the complicated potential provided by a protein, it is not obvious that a semiclassical approach will work. Also, the harmonic treatment of the amplitude fluctuations becomes questionable because of the rapidly varying electron-atom pseudopotentials. This issue is an objective of complementary treatment of ET presented in Sections 4.2 and 4.3.

2. Electron transfer rate theories

2.1. Semiclassical model and quantum-mechanical aspects of ET

To provide a theoretical framework for discussing problems of ET in natural systems, we will briefly recapitulate differences between adiabatic and nonadiabatic transitions in simple chemical reactions (*cf.* [29,10, 9, 20, 30, 21, 31]).

Chemical reactions involve dynamic motions of electrons and nuclei. Because of the mass difference, one can consider the nuclei at any moment to be fixed (Born–Oppenheimer approximation) so that suitable wave functions, $\Psi_k(\{\boldsymbol{X_q}\})$ and corresponding electronic Hamiltonian, $H_{\mathrm{el}}(\{\boldsymbol{X_q}\})$, depend parametrically on the nuclear coordinates $\{\boldsymbol{X_q}\}$. The states before and after the reaction are then described by two different electronic states

of given energies. The transition is considered to take place between an initial electronic state of a system, Ψ_i, in which the electron can be said to be localized in a "donor" region (R) and a final state, Ψ_f, in which an electron has been transferred to a spatially distinct "acceptor" region (P). The various contributions to the transfer dynamics from nuclear and electronic degrees of freedom may be described by classical, semiclassical, or quantum theories [20, 21, 9, 27, 32, 28, 25, 5, 12, 29]. For ET processes occurring in dissipative condensed-phase media, the dynamics can often be cast in the framework of Kramers-like theory [33, 34, 22, 35, 36, 37] as a chemical kinetic process characterized by a diffusion related rate constant k.

Two types of ET processes are commonly distinguished: an intramolecular process in which the reacting sites are considered to be chemically bound (in general, by covalent links to an intervening bridge, *cf.* Section 4.3) and an intermolecular process in which separate reactants R come into contact forming a complex which then reacts yielding separate product species P. In practice, differences between those two types can be dubious. Effective electronic overlap between basins R and P does not necessarily require covalent bonding between reactants and so called "superexchange" models [25, 26, 31] may be applied to more general situations. Some sort of a unified view can be achieved by treating quantum mechanically the reactive complex as a "supermolecule" [38, 21] which comprises species of P and R together with the intervening bridges. A comprehensive treatment of the kinetics must involve, however, the dynamics of the electronic manifold and that of the nuclear modes (*e.g.* translational or orientational diffusion involving the solute or solvent molecules).

If the coupling between the states Ψ_i, Ψ_f exists, two energy curves specific for the different electronic states repel each other giving rise to a splitting:

$$\Delta = 2H_{if} \equiv \langle \Psi_i | H_{\mathrm{el}} | \Psi_f \rangle \,. \tag{2.1}$$

According to a semiclassical model, in which the nuclei move classically and the electronic states adjusts to the changing nuclear coordinates, transition between the states $|i\rangle$ and $|f\rangle$ can occur only through the H_{if} coupling. If $H_{if} = 0$, the system will remain in state $|i\rangle$ because the electronic state cannot change even if the nuclear coordinates, through their thermal motion, will change their configuration to the one characteristic for the state $|f\rangle$. If H_{if} is very large compared to the kinetic energy of nuclear motion, $k_B T$, the electronic state $|f\rangle$ remains thermally inaccessible, and the nuclei will move according to the "lower" electronic state. When $\Delta \leq k_B T$, thermodynamic considerations alone do not determine whether the electronic state can change. Depending on the relative time scale of electronic and nuclear motions, the system can either remain in state $|i\rangle$ or undergo a transition from $|i\rangle$ to $|f\rangle$.

In a non-adiabatic process the system jumps the small gap between the interacting energy surfaces and continues on the same surface, *i.e.*, in an electronic state with the same characteristics as the state of the system before the crossing. The probability of the jump is given by Landau–Zener equation [39]:

$$P = 1 - \exp\left(-\frac{\pi\gamma_{LZ}}{2}\right), \tag{2.2}$$

where the adiabaticity parameter γ_{LZ} is defined as the ratio of the splitting Δ to the energy uncertainty $\hbar/\tau_{LZ}$ and can be written in the form of

$$\gamma_{LZ} = \frac{\Delta^2}{\hbar v|(F_2 - F_1)|}, \tag{2.3}$$

where v is a nuclear velocity and F_1, F_2 stand for the slopes of the non-interacted energy surfaces [4].

Nonadiabatic ET in which there is appreciable nuclear tunneling is conveniently considered in terms of the formalism developed for multiphonon radiationless transitions [40, 5, 20]. In this formalism the probability per unit time that a system in an initial vibronic state iv will undergo a transition to a set of vibronic levels $\{fw\}$ is given by:

$$w = \frac{2\pi H_{if}^2}{\hbar} \sum_w S_{iv,fw}^2 \delta(\varepsilon_{iv} - \varepsilon_{fw}), \tag{2.4}$$

where $S_{iv,fw}$ is the overlap of the vibrational wavefunctions and $\varepsilon_{iv}, \varepsilon_{fw}$ are the energies of the vibrational levels. If a Boltzman distribution over the vibrational energy levels of the initial i state is assumed, the thermally averaged probability per unit time of passing from a set of vibrational levels $\{iv\}$ to a set of vibrational levels $\{fw\}$ of the final state is

$$k_{NA} = \frac{2\pi H_{if}^2}{\hbar}\langle \mathrm{FC}\rangle, \tag{2.5}$$

where

$$\langle \mathrm{FC}\rangle = \frac{1}{Q_i}\sum_v \sum_w \exp\left(-\frac{\varepsilon_{iv}}{RT}\right) S_{iv,fw}^2 \delta(\varepsilon_{iv} - \varepsilon_{fw}) \tag{2.6}$$

[4] Note that Eq. (2.3) verifies the argument given above. For $\gamma_{LZ} \gg 1$, $P = 1$ and the transition is adiabatic whereas for $\gamma_{LZ} \ll 1$, P tends to $\pi\gamma_{LZ}/2$ with a direct proportionality to Δ^2; a typical result for a highly nonadiabatic transition. For common nonadiabatic ET processes $|\Delta| \leq 10^{-3}$ a.u. which is *c.a.* 0.03 eV or *c.a.* 0.6 kcal mol [29, 9 27, 25], so that it becomes critical for the model in use to predict the value of Δ for a given ET reaction).

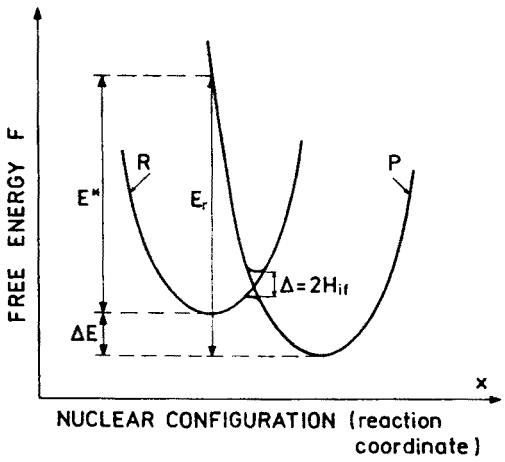

Fig. 2.1. Energy profiles of reactant and product states as a function of the electron-transfer reaction coordinate. The reorganization energy E_r (the vertical difference between the free energies of reactants and products at the equilibrium nuclear configuration of the reactants) is the sum of the reaction energy ΔE (taken as positive for an exothermic process), and the optical excitation energy E^*. Δ is the energy separation between the energy surfaces due to electronic coupling of R and P states. Thermal ET occurs at the nuclear configuration characteristic to the intersection of the curves.

stands for a thermally averaged vibrational overlap (Franck–Condon factor) and

$$Q_i = \sum_v \exp\left(\frac{-\varepsilon_{iv}}{RT}\right) . \tag{2.7}$$

In the high temperature limit $\hbar\omega \ll k_B T$ and by assuming that there is only a single vibrational mode of angular frequency ω undergoing displacement in the ET process, the above equation yields

$$k_{NA} = \frac{H_{if}^2}{\hbar}\left(\frac{\pi}{E_r RT}\right)^2 \exp\left[-\frac{(\Delta E + E_r)^2}{4E_r RT}\right] , \tag{2.8}$$

where E_r is the "reorganization energy" [20, 30] which is equal to the sum of reaction energy ("exothermicity") and the optical excitation energy (*cf.* Fig. 2.1). ΔE stands for the difference of energy between the final and the initial state (negative for a spontaneous reaction). Equation (2.8) is also readily derivable from transition state theory using a Landau–Zener treatment of the barrier crossing Eqs. (2.2), (2.3) with v estimated by the one-way thermal average across the barrier.

2.2. Medium relaxation dynamics and electron transfer

The averaging over the Franck–Condon factor over the thermal equilibrium distribution is permissible only if the medium dynamics (its characteristic relaxation time) is fast on the time scale of ET. For very fast ET rates this may not be the case and one has to correct the previous nonadiabatic result Eq. (2.8) by incorporating explicitly the relaxation time of the environment. The dynamic effect of the "solvent" on activated rate processes was first addressed and consistently treated by Kramers [41]. In Kramers' approach, the reaction system is idealized as an effective Brownian particle moving across in a one-dimensional potential barrier $V(x)$, where x represents a reaction coordinate.[5] The influence of the solvent on the reaction dynamics is described stochastically through a Fokker-Planck Equation (FPE) for the distribution of position x and velocity $\dot{x}$ of the Brownian particle or, equivalently, by a Langevin equation. By incorporating solvent memory effects, Kramers' theory can be generalized, so that effectively the reaction coordinate dynamics is governed by a generalized Langevin equation (GLE):

$$\ddot{x}(t) = -\partial_x V(x) - \int_0^t d\tau \eta(t-\tau)\dot{x}(\tau) + \tilde{F}(t)\,, \tag{2.9}$$

where the random force $\tilde{F}(t)$ is assumed to be a Gaussian process satisfying the fluctuation-dissipation theorem[6]

$$\langle \tilde{F}(t)\tilde{F}(t+\tau)\rangle = 2k_B T\eta(\tau) \tag{2.10}$$

together with the relations:

$$\begin{aligned} \langle \tilde{F}(t)\dot{x}\rangle &= 0\,, \\ \langle \tilde{F}(t)\rangle &= 0\,. \end{aligned} \tag{2.11}$$

---

[5] The time dependent reaction coordinate $x(t)$ for an ET process is commonly identified with a portion of nonequilibrium, orientational polarization for the time-dependent effective charge distribution in the solvent which is assumed to satisfy Eq. (2.9). As such, the reaction coordinate $x(t)$ is a macroscopic variable, a function of a great number of microscopic coordinates characterizing the position and orientation of mutually interacting solvent (medium) molecules.

[6] Relation (2.10) can be understood as a definition of the dissipative memory kernel $\eta(\tau)$.

Though the description of the motion of the effective particle along the reaction path in terms of GLE seems reasonable, it is not rigorous and one encounters difficulties in its use (for the discussion of this issue, see *e.g.*, [42, 43]). First of all, it has not been generally proven that in the presence of an arbitrary potential $V(x)$, Eqs. (2.9), (2.10) can hold simultaneously with Eqs. (2.11). Secondly, the random force $\tilde{F}(t)$ is usually not well specified and may itself be dependent on dynamics of the effective particle in the external field. Therefore in using GLE one makes additional assumptions of questionable validity, such as the Gaussian nature of $\tilde{F}(t)$.

The derivation of a GLE from exact microscopic equations has received much attention [44, 45, 42, 46]. But as discussed in more detail in [42], the formal status of a GLE for a barrier crossing reaction is uncertain [7]. In the special case where all forces in the system are linear, *i.e.*, the GLE is linear in the reaction coordinate $x(t)$ and the potential coupling of the effective particle to the bath is bilinear in x and the coordinates of bath, Eqs. (2.9), (2.10) are exact and derivable from a system Hamiltonian [44, 43, 46].

A complementary method of calculating the rate, especially practical for mathematical analysis is based on derivation of a Fokker–Planck equation (FPE) associated with a non-Markovian Langevin equation. The method is, again, applicable mostly to the situations where the system dynamics can be characterized by harmonic potentials and Gaussian random forces (the only case when the closed-form FPE can be derived from the starting GLE [47, 46, 48]). In the latter case, it is also possible to relate dynamics of the system with only one coordinate in projected phase space [48, 49, 33, 34, 50] whose time evolution can be recast in terms of "generalized (nonstationary) Smoluchowski equation" (GSE).

Such a reduced description of the process, obtained after applying a projection technique leading to a contracted evolution equation GSE yields, however, substantial problem of posing correctly an appropriate boundary condition [18, 51]. In the discussion of this issue, we have also shown [18] that, depending on the method of elimination of auxiliary variables leading to a 1-dim GSE, various forms of diffusion and drift coefficients for the diffusion equation can be derived, which in turn, lead to different long-time predictions of the system dynamics. Evaluation of the rate in this case yields consistent results only in the high friction limit [18] which can be shown to be asymptotically equivalent to a trivial nonmemory dynamics.

---

[7] For the equation to be of practical value, the dynamics entering the time dependent friction should be independent of the external field $V(x)$ and depend only on the dynamics of the pure bath [44, 45, 42, 46].

2.3. *Adiabatic versus nonadiabatic ET processes*

Given relaxation of the medium can be satisfactorily described by Eq. (2.9), the overall electron-transfer rate is determined by the interplay of two factors: the strength of electronic coupling between the states and relaxation dynamics of the solvent (which represents "nuclear degrees of freedom"). Interpolation of the transfer rate between the purely nonadiabatic rate constant Eq. (2.5) and Kramers' prediction [41, 37] for a fully adiabatic reaction

$$k_{AD} = \beta m\omega^2 D \left(\frac{\beta\Delta V^*}{\pi}\right)^{1/2} e^{-\beta\Delta V^*} \tag{2.12}$$

assumes the form [8]:

$$k_{\text{overall}} = (k_{NA} + k_{AD})^{-1} (k_{NA} k_{AD}), \tag{2.13}$$

where D is a "diffusion constant" related to a Brownian dynamics along the reaction coordinate and ΔV^* is the contribution to the free energy of activation from the nuclear reorganization. In a semiclassical model (*cf.* Eq. (2.8))

$$\Delta V^* = \frac{(\Delta E + E_r)^2}{4E_r}. \tag{2.14}$$

For a medium characterized by a single relaxation time τ_L [9] the friction term defined by fluctuation-dissipation relation (2.10) is time independent $\eta = \omega^2\tau_L$ and the diffusion constant can be identified as [33, 34, 35, 36, 22, 43, 18]

$$D = (\beta m\omega^2\tau_L)^{-1} = (\beta m\eta)^{-1}. \tag{2.15}$$

The τ_L dependence of the ET rate can be now recast in the explicit form, Eq. (2.13):

$$k_{\text{overall}}(\tau_L) = \frac{k_{NA}}{1 + \kappa_A}, \tag{2.16}$$

---

[8] Formula (2.12) refers to the case of the overdamped dynamics in a cusp-like potential; a quartic potential with a parabolic barrier top characterized by the barrier frequency ω_b leads to the rate $k_{AD} = \frac{\omega\omega_b}{2\pi\eta} e^{-\beta\Delta V^*}$.

[9] In terms of ET nomenclature, this case corresponds to a Debye solvent, for which the Laplace transform of dielectric response function, $\hat{E}(s) = (1+s\tau_D)^{-1}$ relates to a frequency-independent friction $\hat{\tau}_L(s) = \tau_L = \varepsilon_\infty\tau_D/\varepsilon_0$. $\varepsilon_\infty, \varepsilon_0$ represent high and low-frequency dielectric constants.

where $\kappa_A = k_{NA}/k_{AD}(\tau_L)$ serves as the adiabaticity parameter[10]:

$$\kappa_A = \frac{4\pi H_{if}^2 \tau_L}{\hbar E_r} . \tag{2.17}$$

Consistently with the above description, in the Debeye solvents, relaxation of the reaction coordinate can be characterized by the correlation function

$$\Delta(t) = \frac{\langle x(0)x(t)\rangle}{\langle x^2(0)\rangle}, \tag{2.18}$$

which in the overdamped limit (acceleration term can be neglected at the level of GLE description, *cf.* Eq. (2.9)) leads to a single exponential decay

$$\Delta(t) = e^{-t/\tau_L} , \tag{2.19}$$

which is simply related to the diffusion constant D (*cf.* Eq. (2.15)):

$$D = -\langle x^2(0)\rangle \Delta^{-1}(t)\dot{\Delta}(t) . \tag{2.20}$$

The vast majority of polar solvents exhibit, however, a continuous distribution of dielectric relaxation times [52, 53], so that severe deviations from relation Eq. (2.16) can be expected in such systems. The same state of affairs prevails for ET processes in glasses, proteins and polymers [7, 2, 54, 55, 1].

In a solvent with static disorder, the dielectric relaxation of the microscopic solvent environment of any electron donor-acceptor pair is exponential but inhomogeneity of various relaxation times τ_L sets up a given distribution of $\tau_L, g(\tau_L)$. The observed survival probability of reactants $P(t)$ is an ensemble average of systems with individual rates $k(\tau_L)$:

$$P(t) = \int_0^\infty e^{-k(\tau_L)t} g(\tau_L) d\tau_L . \tag{2.21}$$

---

[10] From Eq. (2.13), if the rate constant for well dynamics is large relative to the rate constant for surface crossing (*i.e.*, $k_{AD} \gg k_{NA}$), then the reactants population is equilibrated and the conventional nonadiabatic rate expression is obtained. On the other hand, when the well motion is sufficiently slow, a dependence on well dynamics (τ_L) will be obtained. Note the difference between κ_A and Landau–Zener adiabaticity parameter Eq. (2.3), the latter being defined for a ballistic motion on the top of barrier between the states of reactants and products.

This issue is further discussed in Section 4.2 where we analyze possibility of the breakdown of the formula for nonadiabatic ET in the presence of an effectively long relaxation time caused by medium inhomogeneity. Quantum mechanical calculations on natural molecules of various configurational states and estimates of configurational costs in biological ET systems are presented in Sections 4.4 and 4.5.

3. Kinetics in a fluctuating potential

3.1. Model of dichotomously changing potential

In this Section we discuss various approaches to study kinetic properties of the system driven by dichotomous forcing. We focus on various definitions of kinetic rates derived from the definition of time-dependent correlation function and analysis of a reaction flux through the barrier separating different stable states.

Description of the model system consists of two factors. First, the full dynamics is expressed in terms of certain set of degrees of freedom $\{x_i\}$. Secondly, action of fluctuating environment is modeled by the set of parameters $\{\alpha_j\}$, which in general can appear nonlinearly in phenomenological equations for time derivative $\dot{x}_i$

$$\dot{x}_i = f(x_i, \alpha_j), \qquad i = 1 \ldots n, \qquad j = 1 \ldots . \tag{3.1}$$

We consider a system whose action is determined by a dichotomously switched potential, *i.e.*, the state of the environment changes between two different levels α_1, α_2 that in turn can be associated with two different potentials V_1, V_2 exerted on a dynamic variable x (for the purpose of simplicity we limit ourselves to a one-dimensional case, although the analysis can be easily extended to many-dimensional space). We assume temporal evolution of α_t to be given by a Markovian dichotomous noise [56]

$$P_{ij}(t) = \mathrm{Prob}(\alpha_t = i \mid \alpha_0 = j), \tag{3.2}$$

where i, j can take on one of two values, $i, j \in \{\alpha_1, \alpha_2\}$. Temporal evolution of the noise depends on λ_1, λ_2 — the mean frequencies of passage from α_1 to α_2 and from α_2 to α_1. Under these assumptions $P_{ij}(t)$ reads

$$P_{ij}(t) = \frac{1}{\lambda_1 + \lambda_2} \begin{pmatrix} \lambda_1 + \lambda_2 e^{-(\lambda_1+\lambda_2)t} & \lambda_1(1 - e^{-(\lambda_1+\lambda_2)t}) \\ \lambda_2(1 - e^{-(\lambda_1+\lambda_2)t}) & \lambda_2 + \lambda_1 e^{-(\lambda_1+\lambda_2)t} \end{pmatrix}. \tag{3.3}$$

A switching of the environment between two different states is a stationary random process with a characteristic correlation function

$$C(t) = \frac{\lambda_1 \lambda_2}{(\lambda_1 + \lambda_2)^2} (\alpha_1 - \alpha_2)^2 \exp(-[\lambda_1 + \lambda_2]t). \tag{3.4}$$

If the environment is in configuration α_i, the equation of motion of x is

$$\frac{dx}{dt} = -\frac{\partial V_i(x)}{\partial x} = f(x, \alpha_i) \equiv f_i(x) . \tag{3.5}$$

The pair process (x_t, α_t) is Markovian and obeys Kolmogorov equation [47]

$$\begin{aligned} \partial_t p(x, \alpha_1, t \mid x_0, \alpha_0, 0) = &- \partial_x f_1(x) p(x, \alpha_1, t \mid x_0, \alpha_0, 0) \\ &- \lambda_1 p(x, \alpha_1, t \mid x_0, \alpha_0, 0) \\ &+ \lambda_2 p(x, \alpha_2, t \mid x_0, \alpha_0, 0) \end{aligned} \tag{3.6}$$

$$\begin{aligned} \partial_t p(x, \alpha_2, t \mid x_0, \alpha_0, 0) = &- \partial_x f_2(x) p(x, \alpha_2, t \mid x_0, \alpha_0, 0) \\ &- \lambda_2 p(x, \alpha_2, t \mid x_0, \alpha_0, 0) \\ &+ \lambda_1 p(x, \alpha_1, t \mid x_0, \alpha_0, 0) . \end{aligned} \tag{3.7}$$

Our interest concerns evolution of the probability density $p(x, t)$ defined as

$$p(x, t) = p(x, \alpha_1, t) + p(x, \alpha_2, t) . \tag{3.8}$$

By assuming statistical independence of the processes x_t, α_t in the infinite past, a closed evolution equation for $p(x, t)$ is [56]

$$\begin{aligned} \partial_t p(x, t) = \int_0^\infty \mathcal{D}(t - t') p(x, t') dt' = &-\partial_x \gamma^{-1} \{\lambda_2 f_1(x) + \lambda_1 f_2(x)\} p(x, t) \\ &+ \partial_x \gamma^{-1} \{f_1(x) - f_2(x)\} \int_{-\infty}^{t} \exp\{-[\gamma + \partial_x \gamma^{-1} (\lambda_1 f_1(x) \\ &+ \lambda_2 f_2(x))](t - t')\} \gamma^{-1} (\lambda_1 \lambda_2) \partial_x \{f_1(x) - f_2(x)\} p(x, t') dt' , \end{aligned} \tag{3.9}$$

where γ stands for the inverse of the noise correlation time

$$\gamma = \lambda_1 + \lambda_2 . \tag{3.10}$$

For a deterministically stable system, well defined stable stationary states to Eq. (3.9) exist, and the stationary probability distribution function $p_s(x)$ is given by [11]

[11] Note that the support of the stochastic process, guaranteeing existence of a positively defined $p_s(x)$ is determined by the union of intervals, whose boundaries are given by zeros of f_1 and f_2.

$$p_s(x) = p_s(x,\infty) = \mathcal{Z}\frac{f_2 - f_1}{f_1 f_2}\exp\left\{-\int^x \left(\frac{\lambda_1}{f_1} + \frac{\lambda_2}{f_2}\right) dy\right\}$$
$$= \mathcal{Z} D_{\text{eff}}^{-1}(x)\exp\left\{-\int^x \frac{H(y)}{D_{\text{eff}}(y)} dy\right\}, \tag{3.11}$$

where $\mathcal{Z}$ stands for the normalization factor. As a direct consequence of the above scheme one gets

$$p(x,\alpha_1,\infty \mid x_0,\alpha_0,0) = \frac{\lambda_1}{\lambda_1+\lambda_2} p(x,\infty)$$
$$p(x,\alpha_2,\infty \mid x_0,\alpha_0,0) = \frac{\lambda_2}{\lambda_1+\lambda_2} p(x,\infty). \tag{3.12}$$

Further information on the steady-state behaviour of the system can be obtained from the extrema of $p_s(x)$ which are solutions to the equation

$$\frac{\partial p_s(x)}{\partial x} = \frac{f_2' f_1^2 - f_1' f_2^2}{f_1 f_2 (f_2 - f_1)} - \frac{\lambda_1 f_2 + \lambda_2 f_1}{f_1 f_2} = 0, \tag{3.13}$$

where

$$f_i' \equiv \frac{df_i}{dx}.$$

For the purpose of further studies it will be convenient also to rewrite Eq. (3.9) in terms of the probability current $j_p(x,t)$ whose Laplace transform fulfills the relation

$$\hat{\mathcal{D}}(s)\hat{p}(x,s) = -\partial_x \hat{j}_p(x,s), \tag{3.14}$$

and

$$\hat{j}_p(x,s) = \gamma^{-1}(\lambda_1 f_2 + \lambda_2 f_1)\hat{p}(x,s)$$
$$+\gamma^{-1}(f_2 - f_1)\left[s + \gamma + \partial_x \gamma^{-1}(\lambda_1 f_1 + \lambda_2 f_2)\right]^{-1} \partial_x (f_1 - f_2)\hat{p}(x,s). \tag{3.15}$$

From Eq. (3.15) we get the following expression for a stationary nonequilibrium current $j_p(x,\infty)$

$$\hat{j}_p(x,0) = \mathcal{F}^{-1}(x)(f_2 - f_1)\int^x dy G(y)\exp\left[-\int_y^x dz \frac{\gamma^2}{\mathcal{F}(z)}\right] \tag{3.16}$$

with

$$\mathcal{F}(x) = \lambda_1 f_1 + \lambda_2 f_2 \,, \tag{3.17}$$

and

$$G(x) = [\gamma + \partial_x \gamma^{-1}(\lambda_1 f_1 + \lambda_2 f_2)] \frac{\lambda_1 f_2 + \lambda_2 f_1}{f_2 - f_1} \hat{p}(x,0) + \frac{\lambda_1 \lambda_2}{\gamma} \partial_x (f_1 - f_2) \hat{p}(x,0) \,. \tag{3.18}$$

3.2. Definitions of transition rates in a system driven by dichotomous noise

There exist few complementary derivations of the kinetic rates [57, 58, 59, 15, 60] of a transition between different stable states of the system described by Eq. (3.9). In the following we will briefly present general formulae for the kinetic rate constant defined for the system driven by dichotomous noise. A generalization of the standard approaches, presented in this Section, assumes that function $f(x,\alpha)$ may be nonlinear both in x and α.

Let us start with a definition of kinetic rate based on estimation of the *escape time*. The measured quantity is an activation current j_0 which starts in a given stable state region and crosses an intermediate region separating two different stable steady states. The forward rate constant between these two states is defined as the inverse of the escape time T [58] of a *metastable* state in the intermediate region. Nonequilibrium current j_0 builds up a total integrated probability p_0 proportional to the escape time T [61]

$$j_0 T = \int_{-\infty}^{\bar{x}_b} p_0(x) dx \,, \tag{3.19}$$

where $\bar{x}_b$ belongs to the intermediate barrier region. By solving Eq. (3.14) for the nonequilibrium p_0 and setting $j_p(x,\infty) = j_0$ we arrive at the formula

$$p_0(x) = j_0 \int_{\bar{x}_b}^{x} \left[\frac{\gamma(f_2(y) - f_1(y)) + f'_1(y) f_2(y) - f'_2(y) f_1(y)}{f_1(y) f_2(y)(f_2(y) - f_1(y))} \right] p_s(y) dy \,. \tag{3.20}$$

Hence the escape rate is [58, 62]

$$r = \frac{1}{2T} = -\frac{1}{2} \left[\int_{-\infty}^{\bar{x}_b} p_s(x) dx \int_{x}^{\bar{x}_b} \frac{1 + (f'_1 f_2 - f'_2 f_1)/(\gamma(f_2 - f_1))}{p_s f_1 f_2 / \gamma} dy \right]^{-1} . \tag{3.21}$$

Another derivation of a phenomenological rate law comes from the standard use of projection operator techniques [45, 44]. Correlation function expressions for the rate constants have then formally a structure similar to those in equilibrium reaction rate theory [3]. We follow directly derivation presented elsewhere [60]. The only generalization made in our approach is that, as it has been stressed before, evolution Eq. (3.9) can be nonlinear not only in x, but also in α-parameter[12]. After [60, 63] we adopt the definition of the *population number in a state of reactants R (or products P)*,

$$N_R(t) = \int_{M_1}^{M_2} p(x,t)\Theta(-x-\delta_1)dx\,,$$

$$N_P(t) = \int_{M_1}^{M_2} p(x,t)\Theta(x-\delta_2)dx\,, \tag{3.22}$$

with its steady-state analogs:

$$\eta_R = \int_{M_1}^{\delta_1} p_s(x)dx\,,$$

$$\eta_P = \int_{\delta_2}^{M_2} p_s(x)dx\,, \tag{3.23}$$

where M_1, M_2 are the roots of $D_{\text{eff}}(x) = 0$ with $M_1 < M_2$ and $\Theta(x)$ represents the Heaviside step function. A state R(P) collects all x belonging to $(M_1, \delta_1), (\delta_2, M_2)$ respectively, and δ_1 and δ_2 are the lower and upper boundary of an intermediate *barrier region.* By use of the projecting operator $\mathcal{P}$

$$\mathcal{P}p(x,t) = p_s(x)\Theta(\delta_1 - x)\int_{M_1}^{\delta_1} p(x,t)dx\eta_R^{-1} + p_s(x)\Theta(x-\delta_2)\int_{\delta_2}^{M_2}\eta_P^{-1}\,, \tag{3.24}$$

and after assuming that the initial distribution $p(x,0)$ is proportional to $p_s(x)$ in each domain R (P) we obtain for the rate

$$\frac{dN_R}{dt} = -\int_0^t \lambda_{RR}(t-t')N_R(t')dt' + \int_0^t \lambda_{RP}(t-t')N_P(t')dt'\,, \tag{3.25}$$

[12] Let us note that in such a case white-noise limit approximation of environmental activity would be meaningless, as it is impossible to define nonlinear operations on a white noise process [56, 47].

with $\lambda_{RR}, \lambda_{RP}$ being definitions of time dependent rate kernels [45, 60]. If the decay time of the population number is long compared with that of the rate kernel and with the noise correlation time $1/\gamma$, one can omit the s dependence of the rate kernel so that the interesting forward rate constant for the reaction going from population of reactants to products[13] is simply $k_f = \hat{\lambda}_{RR}(0)$. From now on, evaluation of $\hat{\lambda}_{RR}$ follows the scheme presented in [60] and requires only a knowledge of analytical expressions for the flux contribution related to this quantity. By use of Eqs. (3.22), (3.23), (3.24), (3.25), $\mathcal{P}$ and its complementary projector, we arrive at

$$k_f = \hat{\lambda}_{RR}(0) = \eta_R^{-1}\left[\int_{\delta_1}^{\delta_2} dx' \frac{1}{\gamma D_{\text{eff}}(x')p_s(x')}\left(\frac{\gamma^2}{f_1 - f_2} + \frac{\mathcal{F}(x')H(x')}{(f_2 - f_1)D_{\text{eff}}(x')}\right)\right.$$
$$\left. + \frac{\mathcal{F}(\delta_2)}{\gamma(f_2(\delta_2) - f_1(\delta_2))D_{\text{eff}}(\delta_2)p_s(\delta_2)} - \frac{\mathcal{F}(\delta_1)}{\gamma(f_2(\delta_1) - f_1(\delta_1))D_{\text{eff}}(\delta_1)p_s(\delta_1)}\right]^{-1}, \tag{3.26}$$

where $H(x)$, $p_s(x)$ and $D_{\text{eff}}(x)$ are defined in Eq. (3.11). The above formula is a natural generalization of the results presented by Kapral *et al.* [60, 63] to the case of multiplicative dichotomous noise affecting the system. One can also use the concept of the mean first passage time MFPT (*i.e.* the average time that a process starting from a point x, inside the initial domain of attraction, needs to reach for the first time the separatrix manifold between R and P regions, [64, 47, 42, 65]). The latter has been derived and elaborated in a series of papers ([37] and references therein) using different boundary conditions. (A natural choice is the requirement of probability absorption at δ_1 and δ_2.) Recently, another method of calculating the rate constant in a dichotomously changing medium has been presented [15, 16], closely related to the stable state picture of Northrup and Hynes [66, 67]. The rate k is expressed in terms of the reactive flux Φ calculated as a long-time derivative of the correlation function:

$$k = \frac{\Phi}{\eta_R}, \tag{3.27}$$

and

$$\Phi = -\lim_{t\to\infty} \frac{dC(t)}{dt}, \tag{3.28}$$

[13] This approach based on a rigorous definition of reactants (R) and products (P) states requires (in the case of multiplicative noise) discussion of existence and relative stability of "noise-induced stationary states", see [16, 56].

where

$$C(t) = \langle N_R(\boldsymbol{x}(0)) N_P(\boldsymbol{x}(t)) \rangle \,, \tag{3.29}$$

so that

$$\Phi = \sum_{\alpha=1,2} \int_S d\sigma(\boldsymbol{x}) \boldsymbol{n}_S(\boldsymbol{x}) \cdot \boldsymbol{J}_\alpha(\boldsymbol{x}) P(\boldsymbol{x}, \alpha) \,, \tag{3.30}$$

where $\boldsymbol{J}_\alpha(\boldsymbol{x}) = \boldsymbol{f}_\alpha(\boldsymbol{x}) p_{\rm st}(\boldsymbol{x}, \alpha)$ is a stationary current, $P(\boldsymbol{x}, \alpha)$ defines the probability to be absorbed in the product region at some time between 0 and ∞ knowing that we started at $t = 0$ at point $\boldsymbol{x}$ with the external environment in configuration α and $\boldsymbol{n}_S$ is the external normal to the hypersurface S at $\boldsymbol{x}$. $p(\boldsymbol{x}, \alpha, t) d\boldsymbol{x}$ is the probability that the process is confined in the volume $d\boldsymbol{x}$ around point $\vec{\boldsymbol{x}}$ and that the external environment is in configuration α at time t. The absorption probability $P(\boldsymbol{x}, \alpha)$ fulfills the equations [15, 16]

$$P(\boldsymbol{x}, \alpha) = P(\boldsymbol{x} + d\boldsymbol{x}_\alpha, \alpha)[1 - \lambda_\alpha dt] + \sum_{\beta,\alpha} P(\boldsymbol{x}, \beta) q_{\alpha,\beta}(\boldsymbol{x}) \lambda_\alpha dt \,, \tag{3.31}$$

which arise from the fact that, when starting from $(\boldsymbol{x}, \alpha)$, there are two ways of being absorbed in the product region. First, the environment does not change its configuration α during the time interval dt (that occurs with probability $1 - \lambda_\alpha(\boldsymbol{x}) dt$) and then the particle moves to point $\boldsymbol{x} + d\boldsymbol{x}_\alpha$, where the deterministic evolution of the system is governed by Eq. (3.5). Second, the environment changes its conformation in time dt which occurs with probability $\lambda_\alpha(\boldsymbol{x})$ and goes to configuration $\beta \neq \alpha$ with probability $q_{\beta,\alpha}(\boldsymbol{x})$. The boundary conditions are:

$$\begin{aligned} P(\boldsymbol{x}, \alpha)|_{x \in \mathcal{P}} &= 1 \quad \text{if} \quad \boldsymbol{n}_P(\boldsymbol{x}) \cdot f(\boldsymbol{x}, \alpha_i) < 0 \,, \\ P(\boldsymbol{x}, \alpha)|_{x \in \mathcal{R}} &= 0 \quad \text{if} \quad \boldsymbol{n}_R(\boldsymbol{x}) \cdot f(\boldsymbol{x}, \alpha_i) < 0 \,. \end{aligned} \tag{3.32}$$

The rate constant given by Eq. (3.27) is a well-defined quantity since it does not depend on the precise choice of the dividing surface (the barrier region), in contrast with the TST constant Eq. (2.8)) (for the discussion, *cf.* [16]).

4. Biophysical applications

4.1. Dichotomic ion channel kinetics

Many biological functions — such as nerve impulses, muscle contractions, vision — have their basis in a sudden change in cell membrane permeability. Specific membrane proteins act as gates or agents of active transport, regulating the flow of molecules and ions between the cell and environment. Members of one class of membrane proteins, the ion channels,

open in response to electrical, chemical or mechanical stimuli to allow the spontaneous flow of ions down a concentration or potential gradient across the cell membrane.

Thermal fluctuations provide energy to cause the proteins to spontaneously alternate between closed conformations that block the flow of ions through the channel and open conformations that permit such a flow [68]. Studies of random fluctuations of the channel current were aimed at understanding the gating mechanism, that is, the changes in conformations that open and close the channel and the processes that affect those changes. Phenomenological models meant to characterize the statistical properties of the experimental data include mostly concepts based on the theory of Markov processes [69, 70, 71], although there is a growing interest in applying methods stemming from the theory of deterministic chaos [72, 73, 54].

As a direct application of the formalism presented in Sections 3.1 and 3.2, let us briefly discuss the model of ionic transport through a gramicidin channel [68, 74, 75]. The model is not a direct exemplification of an ET in biological medium; ion transfer can be safely described as a classical diffusion process with a macroscopic flux of charge-carriers passing through the pore. The expressions derived in this Section can be, however, used in a broader sense applied to estimate the adiabatic factors determining the ET rate in stochastic media.

The gramicidin channel is well-suited for theoretical study because of its structural and functional simplicity. Because it exhibits functional behaviour similar to more complex biological channels, while being relatively small and structurally well characterized, the gramicidin channel serves as the model of choice for studies of the mechanisms of ionic permeation across lipid membranes [68].

Free energy profile $V(X)$ of the gramicidin channel is known [75] to be dominated by relatively long-range, slowly varying electrostatic forces. The energy of a single ion passing through the channel in units of kT is

$$V(x) = V^0(x) + \Psi_{el}(x)\,, \tag{4.1}$$

and represents the sum of single ion energy in the absence of applied voltage [74, 76]

$$V^0(x) = 5.3 - 21.1(x - \tfrac{1}{2})^2 = \delta - \beta(x - \tfrac{1}{2})^2\,, \tag{4.2}$$

and an applied potential gradient at a position[14] x:

$$\Psi_{\mathrm{el}}(x) = A(1 - x)\,. \tag{4.3}$$

[14] Position of an ion x is expressed as a ratio of the distance X from the channel end to channel length L.

In the model, A is assumed to be dichotomously changing switching of the applied potential:

$$A \in \{+\Delta, -\Delta\} + \Delta \underset{\lambda_2}{\overset{\lambda_1}{\rightleftarrows}} -\Delta . \tag{4.4}$$

Steady states of the potential (4.1) are:

$$x_{s_1,s_2} = \frac{1}{2} \pm \frac{\Delta}{2\beta} , \tag{4.5}$$

and we assume $\Delta/\beta > 1$. Regions described previously as R and P (reactants and products) can be now associated with the positions of the ion to the left of $x = 0$ and to the right of $x = 1$, respectively. The intermediate barrier region is located in the neighbourhood of $x = 1/2$. The process of an active transport through the channel takes place in the interval $x \in [0, 1]$ so that it is included within $[x_{s_1}, x_{s_2}]$ limited by natural boundaries that the stochastic process $x(t)$ cannot exceed. The evolution of the dynamical variable $x(t)$ is governed by an Eq. (3.5) or its probabilistic analogue (3.9). The stationary probability that the external environment of the ion is in a state $\Delta(-\Delta)$ is $\lambda_2/(\lambda_2 + \lambda_1), (\lambda_1/(\lambda_1 + \lambda_2))$. These values have meanings similar to channel gating [68] probabilities. In fact, for $A = -\Delta$ the ion is likely not to pass the channel (the channel is "close") and similarly, for $A = +\Delta$, the channel is open for the ion transport. The probability $P(x, \alpha)$ of an ion to be absorbed i n the product region (which is now the interior of the channel of length L) at some time between 0 and ∞ knowing that the process started at time $t = 0$ at point x with the external environment in configuration α fulfills the system of Eqs. (3.27):

$$\begin{aligned} \frac{\partial P(x,1)}{\partial x} &= \frac{\lambda_1}{F_1(x)}[P(x,1) - P(x,2)] , \\ \frac{\partial P(x,2)}{\partial x} &= \frac{\lambda_2}{F_2(x)}[P(x,2) - P(x,1)] \end{aligned} \tag{4.6}$$

with the boundary conditions

$$\begin{aligned} P(a_1 = 0, 2) &= 0 , \\ P(a_2 = 1, 1) &= 1 . \end{aligned} \tag{4.7}$$

To solve Eq. (4.6) we first introduce

$$\Psi(x) = P(x,2) - P(x,1) . \tag{4.8}$$

From Eq. (4.6) we have then

$$\Psi(x) = -P(a_1, 1) \exp\big(t_2(x|a_1) - t_1(a_1|x)\big)\,, \tag{4.9}$$

where $t_\alpha(x|y)$ is defined as

$$t_\alpha(x|y) = \int_y^x \frac{\lambda_\alpha}{F_\alpha(x)} dx, \qquad \alpha = 1, 2\,, \tag{4.10}$$

and we have used

$$\Psi(a_1) = -P(a_1, 1)\,. \tag{4.11}$$

From the first equation of the set (4.6) we get

$$P(x, 1) = P(a_1, 1) + \int_x^{a_1} \frac{\lambda_1}{F_1(x)} \Psi(x) dx\,. \tag{4.12}$$

By setting $x = a_2$ in this equation, we arrive at

$$P(a_1, 1) = \left[1 + \int_{a_1}^{a_2} \frac{\lambda_1}{F_1(x)} \exp\big(t_2(x|a_1) - t_1(a_1|x)\big) dx\right]^{-1}, \tag{4.13}$$

which yields

$$P(a_1 = 0, 1) = \left[1 + \frac{\lambda_1 (2\beta)^{-1+\nu+\mu}}{(\Delta+\beta)^\mu (\Delta-\beta)^\nu} \int_0^1 dx \left|x + \frac{\Delta-\beta}{2\beta}\right|^{\nu-1} \left|x - \frac{\Delta+\beta}{2\beta}\right|^\mu\right]^{-1} \tag{4.14}$$

with $\mu = \lambda_2/2\beta$ and $\nu = \lambda_1/2\beta$, $\mu, \nu > 0$. We now estimate the integral in (4.14) for three characteristic cases (*cf.* Fig. 4.1):

(a) $\lambda_2 = 2\beta, \lambda_1 = \beta, p_1 \equiv \lambda_2/(\lambda_1 + \lambda_2) = 2/3, p_2 \equiv \lambda_1/(\lambda_1 + \lambda_2) = 1/3$ (the channel is "open" for the passing ion)

(b) $\lambda_2 = \beta, \lambda_1 = 2\beta, p_1 = 1/3, p_2 = 2/3$ (the channel is "close")

(c) $\lambda_1 = \lambda_2 = \beta; p_1 = p_2 = 1/2$ (the channel is equally likely to be "open" or "close"for passing ions).

For case (a), Eq. (4.14) takes the form:

$$P(a_1, 1) = \left[1 + \frac{1}{(\Delta+\beta)(\Delta-\beta)^{1/2}} \left[2\Delta(\Delta+\beta)^{1/2} - 2\Delta(\Delta-\beta)^{1/2} - \frac{1}{3}(\Delta+\beta)^{3/2} + \frac{1}{3}(\Delta-\beta)^{3/2}\right]\right]^{-1}. \tag{4.15}$$

In case (b) one gets

$$P(a_1,1)=\left[1+\frac{2}{3(\Delta+\beta)^{1/2}(\Delta-\beta)}\left[(\Delta+\beta)^{3/2}-(\Delta-\beta)^{3/2}\right]\right]^{-1}. \quad (4.16)$$

For the symmetric case (c) $P(a_1,1)$ is

$$P(a_1,1)=\left[1+\frac{\Delta}{(\Delta^2-\beta^2)^{1/2}}\left[\arctan\frac{(\Delta+\beta)^{1/2}}{(\Delta-\beta)^{1/2}}-\arctan\frac{(\Delta-\beta)^{1/2}}{(\Delta+\beta)^{1/2}}\right]\right]^{-1}. \quad (4.17)$$

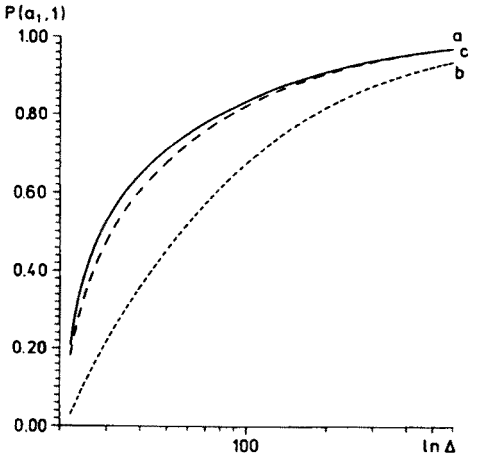

Fig. 4.1. Probability of an ion to be absorbed in the interior of the channel given the external environment has been prepared in a state "1" $(+\Delta)$. (a)$\lambda_1=\beta, \lambda_2=2\beta$; (b)$\lambda_1=2\beta, \lambda_2=\beta$; (c)$\lambda_1=\lambda_2=\beta$.

Patch-clamp recordings from a single ionic channel have proved to be an effective way of extracting information about the conformational states of gating macromolecules. In the studies of some gap junctions [77, 78, 79], patches containing only one channel constitute a minority of recordings. Anatomical studies, mostly freeze fracture, have revealed that individual gap junction channels tend to aggregate in groups, that could explain cooperative behavior observed in their patches. A molecular interpretation of the observed cooperativity can be understood in terms of mechanical interactions between the neighboring channel proteins. We have derived a model [77] which describes the cooperative gating of channels using only the current amplitude histograms for the probability of observing various conductance levels. The process of channel gating is then described in terms

of an aggregated Markov process, *i.e.*, a finite Markov process in continuous time, the states of which are grouped into several aggregates. The composite effect of correlated recordings from various conductance levels can be then easily analyzed in terms of aggregation of proteic monomeric subunits forming conducting $n - mers$.

4.2 Similarities between glasses and proteins. Kinetics in "rough" potentials

Proteins are complex systems owing to their structure and the many competing interactions among their constituent atoms. The primary structure of a protein consists of a linear chain of amino-acids linked by covalent peptide bonds. The chain folds into secondary structure elements, the most important of which are α helices and β-pleated sheets. The helices and sheets fold into a compact three-dimensional tertiary structure which determines the biological activity of the protein molecule. Unlike the situation in crystalline solids, the absence of obvious spatial symmetries in a protein molecule does not force the molecule into a unique structure. The comparatively weak forces that stabilize the protein allow for considerable structural variability [1, 80]. Led by this observation, Klotz and Weber [81] suggested that a protein with a given primary sequence exists in many conformational states that are dynamic in nature. Functional relevance of the manifold of protein conformational states has been established experimentally in flash photolysis studies of *e.g.*, small ligand binding to myoglobin by Frauenfelder *et al.* [82, 6]. The existence of states and substates implies two types of motion in proteins — equilibrium fluctuations and functionally important motions which are nonequilibrium processes driving the system from one functional state to the another.

Interpretations of the flash photolysis experiments on proteins led some authors [82, 83] to the conclusion that substates and fluctuations in proteins posses a hierarchical character which results in a nonexponential relaxation. It has been well recognized that the relaxation time follows an unusual law (the Vogel-Fulcher Law, [84, 54, 73]) and can be correlated with some characteristic (not necessarily Gaussian) distribution in kinetic parameters. Similar conclusion can be drawn from the theoretical models of photosynthetic chromophores [85, 86, 13, 17]. The molecular dynamics calculations performed on photosynthetic conformers and their natural models [87, 88, 19] suggest that they possess high structural flexibility with relatively low steric energy differences between various conformational forms.

A particular aspect of biopolymers is also the usual presence of the hydration shell, a monolayer or two of bound water molecules on the surface of the protein. In heme proteins, the hydration shell displays a broad liquid-glass like transition [1, 80, 2], which in turn can be characterized by

general features displayed by this class of transitions studied in amorphous materials. The most significant points are the divergence of the transport or inverse transport properties (such as viscosity, inverse diffusion constant and relaxation times) and the extremely broad relaxation phenomena of the stress and modulus.

This experimental and theoretical picture led us to explore further the combined effect of both steric and electronic factors resulting from conformational variability of chromophores on the kinetic rate of ET processes in proteins [19, 13]. On the basis of a simple model presented below, we infer the possibility of longer effective relaxation times in a spatially disordered medium, which can eventually lead to the breakdown of the nonadiabatic limit and question a direct applicability of a conventional kinetic rate approach.

The general nonadiabatic system used for description of a fast long-range ET consists of a two-level system coupled to a reaction coordinate (*cf.* Section 2). Time–evolution of the reactants' population can be viewed in terms of time-dependent properties of the diagonal elements of the density matrix ρ relevant for that problem. By adopting the coarse-grained kinetics for the diagonal elements of ρ introduced by Zusman [33, 34], the evolution equations for the system become

$$\partial_t \rho_R(x,t) = -H_{RP}(x,t)\delta(x - x_{cr}) + L_R \rho_R(x,t)\,, \tag{4.18}$$

$$\partial_t \rho_P(x,t) = H_{RP}(x,t)\delta(x - x_{cr}) + L_P \rho_P(x,t)\,, \tag{4.19}$$

$$H_{RP} = \frac{2\pi H_{if}^2}{\hbar}[\rho_R(x,t) - \rho_P(x,t)]\,, \tag{4.20}$$

$$x(t) \equiv \Delta E_{RP}(t) - \langle \Delta E_{RP}(t) \rangle = \delta E_{RP}(t)\,, \tag{4.21}$$

where $\rho_R(x,t)$ stands for the probability distribution function for the reaction coordinate x value [15] at time t to belong to the "reactants" or "products" wells, respectively, H_{RP} represents the electronic coupling between the two diabatic surfaces and $L_{R,P}$ is a Liouvillean operator for the classical diffusive motion within the harmonic well. If the dynamic properties of

[15] In the original Zusman's approach [33], the reaction coordinate is defined as time-dependent energy gap between the levels of a two-state system, *cf.* Eq. (4.21). That yields ρ as an explicit function of energy. Conversion to any generally chosen "reaction coordinate" y would require scaling of ρ according to $\rho(x,t)dx = \rho(y,t)dy$, which yields $H_{RP} = 2\pi H_{ij}^2(\hbar a y_0)^{-1} \times [\rho_R(y,t) - \rho_P(y,t)]$, where the spring constant a relates solvent polarization mass to the curvature of the well $a = m_L\omega_L^2 = 2E_r/y_0^2$, y_0 being the minimum of the reactants' parabola.

the medium described by $L_{R,P}$ can be approximated by the overdamped[16] Debye solvent, $L_{R,P}$ takes the form of the Smoluchowski operator

$$L_R = \tau_L^{-1}\left(\frac{\partial}{\partial x}x + \langle x^2\rangle_{\rm eq}\frac{\partial^2}{\partial x^2}\right),$$
$$L_P = \tau_L^{-1}\left(\frac{\partial}{\partial x}(x - 2E_r) + \langle x^2\rangle_{\rm eq}\frac{\partial^2}{\partial x^2}\right), \tag{4.22}$$

where E_r represents the reorganization energy of the solvent and τ_L stands for a characteristic longitudinal relaxation time of the medium, related to the friction coefficient η by the formula Eq. (2.15).

For a non-Debye solvent, Liouvillean will be explicitly time-dependent but with the assumption of the overdamped motion within the well, solvent relaxation can be characterized in terms of a finite number of exponentials, so that one can choose an equivalent "effective", time independent Liouvillean to describe rate-limiting diffusive dynamics of the solvent [35, 22, 52]. Eqs. (4.21) can be solved by use of the Laplace-transform technique with a suitably chosen initial conditions (the usual assumption is that at time $t = 0$, the system resides in either one of two diabatic states with the equilibrium distribution $\rho_{\rm eq}$). The time evolution of variations

$$\delta\rho_R(t) = \rho_R(t) - \rho_{\rm eq} \tag{4.23}$$

is given by

$$\frac{d}{dt}\delta\rho_R(t) = -\int_0^t d\tau k_{rxn}(\tau)\delta\rho_R(t-\tau), \tag{4.24}$$

and in the overdamped limit, after assuming the Debye representation of the solvent, leads to the Kramers expression (*cf.* Eq. (2.12)) for the rate k_{rxn}

$$k_{rxn} \equiv k_{AD} = \tau_L^{-1}\left(\frac{\beta V(x^*)}{\pi}\right)^{1/2} e^{-\beta V(x^*)}. \tag{4.25}$$

The above formula is within 10% exact for sufficiently high barriers (*i.e.* $\beta V(x^*) \geq 5$, where $\beta V(x^*)$ stands for the parabolic potential value at the top of the barrier. For lower barriers, k_{rxn} has to be corrected by a

[16] Assumption of the overdamped dynamics is essential for the purpose of using the particular form of the kinetic rate (effective Kramers limit). The general variational state theory [89] which is also a suitable theory in the case of cusplike potentials, predicts deviations from the rate (Eq. (2.8)) beyond the strong-damping limit.

multiplying factor $\Psi(z) = (1 + \mathrm{erf}(z))[ze^{-z^2} \int_{-\infty}^{z} dxe^{x^2}(1 + \mathrm{erf}(x))^2]^{-1}$, $z = \beta V(x^*)$).

The point we want to make now is that given the local fluctuation in steric effects of the potential can be represented in the form of Gaussian-distributed "ripples" imposed on the otherwise smooth, averaged potential surface, the effective relaxation time for the medium becomes exponentially enhanced. Let us start our description by use of the thermodynamic concept of the amorphous state. An amorphous state is a random but frozen state. Suppose that the total energy for the system is

$$H = H_0 + H_1\,, \tag{4.26}$$

where H_0 stands for the background "solvent" energy with the random structure of "impurities". Interactions between the "background" and the impurities and among the impurities themselves yield an extra term in the energy Eq. (4.26) of the system. The total thermodynamic potential (free energy function) for the system can be calculated by use of the partition function:

$$\begin{aligned} e^{-\beta V} &= \sum_x e^{-\beta(H_0(x)+H_1(x))} \\ &= e^{-\beta V_0} e^{-\beta \Phi(x)}\,, \end{aligned} \tag{4.27}$$

where x stands for some collective coordinate in the system. From Eq. (4.27) one gets

$$\frac{\sum_x e^{-\beta(H_0(x)+H_1(x))}}{\sum_x e^{-\beta H_0(x)}} = \langle e^{-\beta H_1(x)} \rangle_{H_0} = e^{-\beta \Phi(x)} \tag{4.28}$$

so that eventually the free energy function can be expressed as

$$V = V_0 - k_B T \ln \langle e^{-\beta H_1(x)} \rangle_{H_0}\,. \tag{4.29}$$

A similar analysis can be repeated in the case of the diffusive well dynamics described by the Liouvillean operator in Eq. (4.21). In this coarse-grained approach, our knowledge of particular types of hamiltonians governing the evolution of "solvent" and "imperfections" dynamics is limited; we are assuming that the free energy potential can be described as a sum

$$V(x) = V_0(x) + f(x)\,, \tag{4.30}$$

where $f(x)$ stands for random, local variations of the potential $V_0(x)$[17]. To calculate the population within the well we need to estimate the integral

$$\int dx e^{-\beta V(x)} \cong \int dx e^{-\beta V_0(x)} \langle e^{-\beta f(x)} \rangle , \tag{4.31}$$

which evaluated over small "distances" dx provides smoothing of $V(x)$. Eq. (4.31) suggests description of the diffusive dynamics in terms of the effective potential

$$V_{\text{eff}} = V_0 - k_B T \ln \langle e^{-\beta f(x)} \rangle . \tag{4.32}$$

From the general form of the Smoluchowski operator Eq. (4.22) we can infer that an effective diffusion coefficient changes to the value (the result is straightforward if the amplitude of fluctuations $f(x)$ does not depend on the coordinate x, for the discussion of more general cases, see [84])

$$\begin{aligned} D_{\text{eff}} &= \left(\langle e^{\beta f(x)} \rangle \frac{1}{D} \langle^{-\beta f(x)} \rangle \right)^{-1} \\ D &= (\beta m_L \omega_L^2 \tau_L)^{-1} , \end{aligned} \tag{4.33}$$

which together with the expression Eq. (4.32) define a classical Liouvillean averaged over random contributions to the potential, $f(x)$

$$L_{\text{eff}} = D_{\text{eff}} \left(\frac{\partial^2}{\partial x^2} + \frac{\partial}{\partial x} V_{\text{eff}} \right) . \tag{4.34}$$

The formal expression for the diffusive rate constant within the harmonic well with randomly distributed "roughness" follows derivation based on the mean first passage time approach [90, 65], with a reflecting boundary condition at $x = -\infty$ and an absorbing boundary at the top of the barrier, $x = x^*$

$$\langle k_{\text{diff}}^{-1} \rangle = \int_{x^*}^{x} dy e^{\beta V_{\text{eff}}(y)} D_{\text{eff}}^{-1} \int_{-\infty}^{y} dz e^{-\beta V_{\text{eff}}(z)} . \tag{4.35}$$

By assuming that the fluctuations $f(x)$ superimposed over the mean potential $V_0(x)$ are Gaussian distributed with a zero mean and dispersion σ^2 direct evaluation of Eqs. (4.32), (4.33), (4.35) with the relaxation rate in the mean potential well predicted by Eq. (4.25) yields

$$\langle k_{\text{diff}}^{-1} \rangle = \frac{e^{\beta^2 \sigma^2}}{k_{rxn}(V_0)} \tag{4.36}$$

---

[17] The dominant contribution in Eq. (4.30) comes from $V(x)$, the amplitude of the perturbation term, $f(x)$ is a measure of the roughness of the potential.

so that duration of the process becomes exponentially enhanced. Note, that the result can be interpreted as the effective enhancement of the longitudinal relaxation time of the medium which can be now expressed as

$$\tau_L^{\text{eff}} = \tau_L e^{\beta^2\sigma^2} = \tau_L e^{T_0^2/T^2}, \tag{4.37}$$

where we have identified $\langle f^2\rangle = k_B^2 T_0^2$. Such forms of the relaxation times have been discussed in temperature-dependent dynamics of spin-glasses [2, 1, 54]. For a Poisson distribution of $f(x)$, same analysis leads to

$$\tau_L^{\text{eff}} = \frac{\tau_L}{1-\beta^2\langle f\rangle^2} = \frac{\tau_L}{1-T_0^2/T^2}, \tag{4.38}$$

predicting a "phase change" at a specific temperature at which τ_L^{eff} diverges. The result differs from the evaluation of the average escape time in a system of random energy barriers, as reported by Vilgis [55], where no underlying structure of the smooth free energy (a potential well) was used in presentation of the model. A direct observation which follows from the derivation of formula (4.35) is that the distribution of first passage times is no longer exponential (*cf.* [55, 84, 7, 54]). The moments of first passage time in the system described by a Liouville equation with a Smoluchowski operator (4.22) can be calculated from the general formulae [64, 90, 47] after substituting potential and diffusion terms with the effective potential (4.32) and the effective diffusion coefficient (4.33), respectively:

$$M_j = 2j \int_{x^*}^{x} dy e^{\beta V_{\text{eff}}(y)} D_{\text{eff}}^{-1} \int_{-\infty}^{y} dz e^{-\beta V_{\text{eff}}(z)} M_{j-1}(z), \tag{4.39}$$

$$M_1 = \langle k_{\text{diff}}^{-1}\rangle, \tag{4.40}$$

and due to the dispersion caused by the randomness of $f(x)$ do not follow the law of the exponential distribution

$$M_j \neq \frac{j!}{M_1^j}. \tag{4.41}$$

In this context, diffusive decay of the population within the harmonic well with a superimposed random roughness would result in nonexponential dynamics. From Eqs. (4.37), (4.38) it becomes apparent that at high temperatures compared to the intensity of fluctuations σ, diffusion within the free-energy well is essentially unaffected by the existence of randomly distributed barriers. At lower temperatures, effective relaxation time will strongly depend on the form of distribution of $f(x)$.

This picture is essentially consistent with the model of a statistical distribution of thermodynamic driving forces in mutated protein ET systems [85, 86]. In fact, by assuming that the "reactants" and "products" free energy potentials are slightly modified by random distribution of "ripples" (reflecting existence of conformational substates in the proteic medium) around their parabolic envelope and do not change their curvature due to ET process, one gets (*cf.* Eqs. (4.30), (4.32) and Fig. 2.1):

$$\begin{aligned} V_R &= a\frac{x^2}{2} + \sigma_1 f_1(x)\,, \\ V_P &= a\frac{(x-b)^2}{2} + \sigma_2 f_2(x) - \Delta V\,, \\ b^2 &= \frac{2E_r}{a}\,, \end{aligned} \tag{4.42}$$

where the "effective" free energy gap between the reactants and products state (defined as the energy difference between the bottoms of the parabolas) becomes a random variable.

If the free energy gap $V_R - V_P = \Delta\tilde{V}$ can be described by a Gaussian distribution around the mean value ΔV, the time evolution of the donor population becomes

$$N_P(t) = N_P(0) \int_{-\infty}^{+\infty} e^{-tk_{NA}(\Delta\tilde{V})}(2\pi\tilde{\sigma}^2)^{-1/2} e^{-(\Delta\tilde{V}-\Delta V)^2/2\tilde{\sigma}^2} d(\Delta\tilde{V})\,. \tag{4.43}$$

The inverse of the average lifetime of the donor state can be then calculated from the above formula leading to a simple expression for the ET rate[18]

$$k = \left[\int_0^{\infty} N_P(t)dt\right]^{-1}\,. \tag{4.44}$$

The result is different from the "average kinetic rate" evaluated as

$$\langle k\rangle = \int_{-\infty}^{+\infty} k_{NA}(\Delta\tilde{V})(2\pi\tilde{\sigma}^2)^{-1/2} e^{-(\Delta\tilde{V}-\Delta V)^2/2\tilde{\sigma}^2} d(\Delta\tilde{V})\,, \tag{4.45}$$

with k_{NA} given by Eq. (2.8).

---

[18] This step requires that a particular form of k_{NA} is known, *e.g.*, the high temperature TST approximation, Eq. (2.8).

Our analysis shows that when applied to the theory of ET in proteic media, this feature would be responsible for an effective enhancement of a longitudinal relaxation time of the medium, which in turn may affect nonadiabatic character[19] of the process (*cf.* Eqs. (2.16), (2.17)). On the other hand, the breakdown of the nonadiabatic limit in the presence of a relatively long relaxation time of the medium, rises the question of a direct applicability of a conventional kinetic rate approach [20].

4.3. Conformational changes of reagents. Concept of fluctuating barriers

Kinetics in ET processes is controlled in part by the behaviour of the near-neighbour electronic couplings which are functions of nuclear coordinates and depend exponentially on the distance between the adjacent chromophores. If the timescale for intermolecular motions is similar to that of the ET transfer time, the electron transfer occurs as a process involving dynamical disorder.

From the point of view of a physical description of the system, the process can be pictured as a "gated" barrier crossing where the height of barrier is fluctuating randomly in time [59, 91, 92, 93]. The process of that type is known to control the flow of small ligand molecules (O_2, CO) into large biomolecules such as myoglobin [1] and has applications to interstitial diffusion in solids [94]. Dynamical disorder is also responsible for a decay of the photoexcited state in the special pair of natural photosynthetic reaction centers [13, 87, 83] (*cf.* Section 4.4, 4.5).

In modelling non-exponential decay of illuminated donor complex of $(BChl)_2$ in reaction centers of purple bacteria *Rhodopseudomonas viridis* (see section 4.5 and [19]), we have assumed that the relaxation process occurs in a fluctuating medium, with a competitive process of isomerization ("dynamic disorder") in which the complex undergoes conformational variations on the time scale of the decay. Spontaneous isomerization of chromophores causing the transition from one configurational state to another one and back has been suggested based on visible variations of the electro-

---

[19] The criterion of adiabaticity Eq. (2.17) requires that the energy uncertainty of the system in the mixing region (close to a transition point) is small compared to the splitting of energy levels within the region. For a diffusive motion along the reaction coordinate, the adiabaticity parameter can be estimated from the residence time in the transition region.

[20] A typical assignment for use of the rate theory is the assumption of excitations and relaxations of nuclear medium modes following the faster time-scale than the electronic ET transfer. This situation calls for a perfect time-scale separation in the system, the limit which does not need to be achieved in a slowly relaxing media.

static energy of chromophores studied in molecular dynamics models of the complex. The time T_i the donor exists in a given configuration i before flipping to the another one has been assumed to follow an exponential law:

$$\text{Prob}(T_i > t) = e^{-\lambda_i t} \qquad \lambda_i > 0, \qquad i = 1, 2 \ldots N\,. \tag{4.46}$$

At the macroscopic level, time variations of the population of the excited donor state $\mathrm{R}^* = (\mathrm{BChl})_2^*$ are governed by phenomenological kinetic equations:

$$\frac{dx}{dt} = -k_{rxn}x - I_t x, \qquad I_t = \{\Delta_i\}, \qquad i = 1, 2, \ldots N\,, \tag{4.47}$$

where I_t describes the process of stochastic changes among various conformations and $x(t)$ stands for the population of the primary donor. Since the pair process $\{x(t), I_t\}$ is Markovian, it is possible to derive an evolution equation for the probability density $p(x, I_t, t)$. Average over I_t yields equation for $p(x,t)$ alone but results also in an explicit memory kernel in the evolution equation for that quantity. A particularly simple form of the evolution equation (3.9) is derived if the conformational changes can be parametrized by two states with a symmetric stationary probability of occupation of a given state:

$$\partial_t p(x,t) = \partial_x k_{rxn} x p(x,t) + \partial_x \Delta^2 x \int_{-\infty}^{t} \exp\{-[\gamma - \partial_x k_{rxn} x](t-t')\}\partial_x x p(x,t')dt'\,, \tag{4.48}$$

where

$$\Delta_1 = -|\Delta_2| = \Delta, \qquad \langle I_t \rangle = 0, \langle I_t I_{t+\tau} \rangle = \Delta^2 e^{-\gamma\tau}\,, \tag{4.49}$$

and

$$\lambda_1 = \lambda_2 = \gamma/2\,. \tag{4.50}$$

The moments of the normalized population $X(t) = x(t)/x(0)$ can be calculated by use of the characteristic function for the process I_t [90, 47] leading to the formula:

$$\langle X^n(t) \rangle = e^{-nk_{rxn}t} e^{-\gamma t/2}\left[\cosh(\Gamma_n t) + \frac{\gamma}{2\Gamma_n}\sinh(\Gamma_n t)\right]$$
$$\Gamma_n = \tfrac{1}{2}(\gamma^2 + 4n^2\Delta^2)^{1/2}\,, \tag{4.51}$$

where positivity of the rate requires $\Delta < k_{rxn}$. Decay of $X(t)$ is no longer governed by a single exponential (*cf.* Figs. 4.2, 4.3), which would be a limiting case if the effect of the fluctuating medium could be ignored.

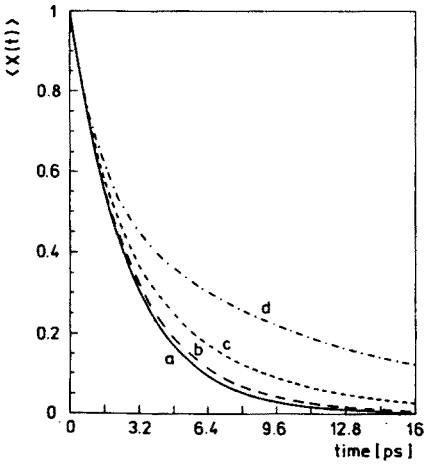

Fig. 4.2. Survival of the average normalized population $\langle X(t)\rangle$ (see the text) as a function of Δ: (a) $\Delta = \gamma = 0, k_{rxn} = 0.37\text{ps}^{-1}$; (b) $\Delta = 0.1$; (c) $\Delta = 0.2$; (d) $\Delta = 0.3$. Curves (b)–(d) are parametrized by $k = 0.37\text{ps}^{-1}$ and $\gamma = 0.05$.

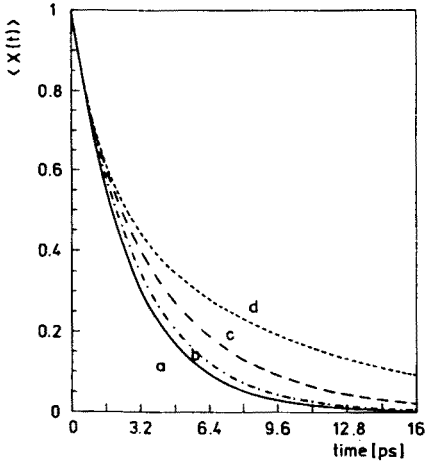

Fig. 4.3. Survival of the average normalized population $\langle X(t)\rangle$ (see the text) as a function of γ: (a) $\Delta = \gamma = 0, k_{rxn} = 0.37\text{ps}^{-1}$; (b) $\gamma = 2.0$; (c) $\gamma = 0.5$; (d) $\gamma = 0.1$. Curves (b)–(d) are parametrized by $k = 0.37\text{ps}^{-1}$ and $\Delta = 0.3$.

An effective relaxation rate for the decay of R* can be defined in terms of the linear relaxation time for a nonlinear process $\langle X(t)\rangle$:

$$k_{\text{eff}} = \tau_{\text{eff}}^{-1} = -\langle X(t)\rangle^{-1} \frac{d\langle X(t)\rangle}{dt}, \tag{4.52}$$

which, together with (4.51) yields:

$$k_{\text{eff}} = k_{rxn} + \frac{\gamma}{2} - \Gamma \frac{\gamma \cosh(\Gamma t) + 2\Gamma \sinh(\Gamma t)}{\gamma \sinh(\Gamma t) + 2\Gamma \cosh(\Gamma t)}$$
$$\Gamma \equiv \Gamma_1 . \tag{4.53}$$

In the limit of short times, $t \to 0$, k_{eff} tends to a "deterministic" value, $k_{\text{eff}} = k_{rxn}$, whereas for $t \to \infty$

$$k_{\text{eff}} = k_{rxn} + \frac{\gamma}{2} - \Gamma$$
$$= k_{rxn} + \frac{\gamma}{2} - \frac{1}{2}(\gamma^2 + 4\Delta^2)^{1/2} < k_{rxn} . \tag{4.54}$$

So that the stochastic dynamics underlying decay of the photoexcited state R^* decreases the relaxation compared with a single exponential deterministic rate k_{rxn}. The difference becomes small for larger values of γ. For large values of γ, Eq. (4.51) yields:

$$\langle X(t) \rangle \approx e^{-k_{rxn}t} \left(1 + \frac{\Delta^2 t}{\gamma}\right) , \tag{4.55}$$

with time-dependent dispersion

$$\sigma_X^2(t) = \langle X^2(t) \rangle - \langle X(t) \rangle^2 \approx \frac{2t\Delta^2}{\gamma} e^{-2k_{rxn}t} . \tag{4.56}$$

From the normalized decay curve of $\langle X(t) \rangle$ one can calculate an average relaxation time

$$\langle \tau \rangle = \int_0^\infty dt \langle X(t) \rangle = \frac{k_{rxn} + \gamma}{(k_{rxn} + \gamma)k_{rxn} - \Delta^2} , \tag{4.57}$$

which can be used to estimate an effective quantum yield ϕ

$$\phi \equiv \frac{\langle \tau \rangle^{-1}}{\langle \tau \rangle^{-1} + \tau_{npc}^{-1}} , \tag{4.58}$$

where τ_{npc} stands for the inverse rate of the non-photochemical process which competes with the ET. Fig. 4.4 displays ϕ as a function of interconversion frequency γ for different values of the noise intensity Δ. Within the range of chosen parameters γ and Δ (*i.e.* those, which ensure the positivity of the overall relaxation rate of the process), quantum yield decays with the

higher values of noise intensities and remains close to unity for increasing values of γ. As it stands, the model can be easily translated to a model of a fluctuating barrier [59, 91, 95] by rewriting Eq. (4.47) in the form

$$\frac{dx}{dt} = -(k_{rxn} + I_t)x = \kappa e^{-\beta\Delta V^*(t)}x = \kappa e^{-A-B\xi(t)}x$$
$$= -\kappa e^{-A}(\cosh B - \xi(t)\sinh B)x\,, \tag{4.59}$$

where $\xi(t)$ stands for a symmetric dichotomous noise. In the limit $\gamma \to \infty$, $\Delta \to \infty$, $\Delta^2/\gamma = \text{const.}$, the dichotomous process tends to a Gaussian white noise producing effective Gaussian statistics of the fluctuating barriers (*cf.* Section 4.1).

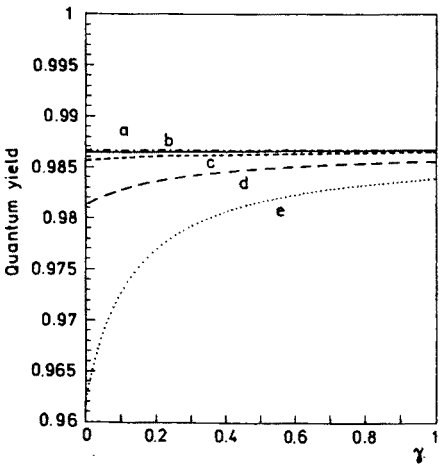

Fig. 4.4. Quantum yield for the process as estimated from Eq. (4.58). For all curves $k_{rxn} = 0.37\text{ps}^{-1}$: (a) $\Delta = 0.01$; (b) $\Delta = 0.05$; (c) $\Delta = 0.1$; (d) $\Delta = 0.2$; (e) $\Delta = 0.3$.

4.4. Diffusive ET tunneling in proteins

Electron transfer (ET) occurs over relatively long distances in a variety of systems. Experimental measurements of electron transfer rates in biological and non-biological materials suggest that as the distance between the donor and acceptor increases, the interaction matrix element becomes dependent on the nature of the intervening medium [96, 25, 26, 9, 27]. Several methods have been proposed [10, 26, 9, 97, 98] to correlate the electronic structure of the transfer-mediating material (molecular "bridges" linking the donor and acceptor or "spacers" distributed within the donor-acceptor

distance) with the intensity of the effective transfer coupling H_{if} controlling interaction between the chromophores. The usual prediction based on experimental evidence is that H_{if} decays exponentially with the number of spacer units. Conventional ET theory assumes that the electronic coupling depends only on the donor-acceptor distance but not on the nuclear coordinates. As a result, the coupling term in the "golden rule" expression for the rate can be separated from the Franck–Condon factor (FC) which contains only thermally weighted overlap integrals of nuclear coordinates (*cf.* Eq. (2.5)). The Condon approximation is valid for intramolecular ET in systems with a rigid spacer, but it becomes questionable for intermolecular ET in soft, flexible media [21, 99, 100]. Because the coupling term is believed to fall off rapidly with distance, McConnell [101] proposed a superexchange model which describes the medium as a source of virtual states for the long-range electronic coupling. For media characterized by a natural accessibility of various configurations (which is the case of ET in proteins), the electronic coupling can fluctuate in time along with the mobile spacer or the solvent.

For electron carriers bond to a protein, long range interactions may be viewed as occurring by a superexchange mechanism through the states in which amino-acid side chains are "oxidized" or "reduced". The distance dependence of bond mediated interactions is determined primarily by the atom types and bond lengths in the transfer mediating bridge [30, 100, 9] which can be composed of aromatic side groups, peptide chains, porphyrin groups or just open gaps. The main strategy in understanding the transfer process is then to search for a dominant set of bonded and nonbonded interactions within the thousands of protein orbitals. In some cases (*cf.* [25, 99]), it is possible to dissect the interactions into "pathways", smaller subsets of protein orbitals or effective orbitals.

The ET tunneling matrix element is proportional to the amplitude of the donor localized wave function which propagates to the acceptor site. Therefore, the product of the factors by which the wave function falls off for each block in a pathway is also proportional to H_{if} and prefactors associated with details of the structure of the donor and acceptor determine its numerical value. For example, a reasonable approximation for estimating wave function decay along the peptide backbone of a protein is [1, 9, 27] to calculate the product of decays for individual CC, CN and OH bonds.

Essentially, H_{if} can be viewed then as the sum of contributions from all possible pathways linking the donor and acceptor. Superposition of the pathways can effectively have both constructive and destructive interference. Beratan, Onuchic and Hopfield [10] have suggested a model of long-range ET in proteins which focuses on chains of chemical bonds that form routes between the chromophores. The coupling mechanism is formulated in terms

of states in which one electron is added to or removed from one of the intervening bonds. The authors derived expressions for the spreading of an electron onto and off neighboring bonds, and for the attenuation of the wave function at each succeeding bond in the pathway. Coupling along a single pathway composed of N_B covalent bonds and N_S noncovalent links has been assumed [9] to have the form of:

$$H_{if}^0 = \frac{\beta_i \beta_f}{E} \prod_{l=1}^{N_B} \varepsilon_c(l) \prod_{j=1}^{N_S} \varepsilon_{nc}(j) . \tag{4.60}$$

Where β 's stand for the exchange parameters, E is the energy measured with respect to the first orbital (bond) that the donor interacts with, and ε describes the decay of a donor wave function along one of the N_c covalent bonds (ε_c) or one of the N_S noncovalent links (ε_{nc}).

Fluctuations of the distance between the orbitals of the bridge which assist ET have been pointed out elsewhere [97, 87, 14] as a possible origin of a new temperature dependence of the rate. A temperature dependent electronic factor reflecting temperature-induced conformational changes has been invoked to explain the significant deviation that is sometimes observed between the calculated and measured rate temperature dependence of activationless processes.

The distance dependence of bond mediated interactions is determined primarily by the atom types and bond lengths in the bridge (*cf.* also Section 4.5). If the appropriate weighted average of the donor and acceptor orbital energies (determined by Franck–Condon approximation) is considerably closer to the highest occupied bonding orbital energy than the lowest unoccupied antibonding orbital energy of an isolated bridge, the charge-transfer process is dominated by a "hole transport". If the energy is closer to the lowest antibonding states of the linker, the dominant part of the process is the electron transport. Depending on whether the electron or hole tunnelling limit is valid, one expects a different relation between the decay of the donor-acceptor interaction with distance in a forward photoinitiated electron transfer compared to the reverse charge recombination. For large donor-acceptor distances and in the case of linear bridge comprised of identical repeating units, H_{if} decays approximately exponentially with distance and depends strongly on the topology and energetics of the linker [14, 10, 99]. The situation becomes especially complex in proteic media which are known to possess many conformational states. Such conformational changes may precede or follow the actual electron transfer and can lead to directional electron transfer in biological systems. Also, the distance fluctuations within the bonded and nonbonded links in the donor-acceptor space can affect the rate and its temperature dependence. In our formulation of the problem [14], we recall the H_{if} coupling element Eq. (4.60) as

derived in the phenomenological analysis of Beratan *et al.* [10] based on a Born–Oppenheimer separation for nuclear modes. The ET rate can be written as

$$k_{NA} = \frac{2\pi}{\hbar} \sum_I B_I \sum_F |\langle \Psi_I | H^{\text{int}} | \Psi_F \rangle|^2 \delta(E_I - E_F), \tag{4.61}$$

where B_I stands for the statistical weight of initial states, E_I and E_F represent energies of initial and final states, respectively and we have assumed that the relaxation times of all nuclear modes coupled to the problem are fast. The initial and final states involved in the ET event are:

$$\Psi_I = \Psi_R(x, y_R, y_P)\chi_i^R(y_R)\chi_j^P(y_P)\Phi_k(y_N), \tag{4.62}$$

$$\Psi_F = \Psi_P(x, y_R, y_P)\chi_{i'}^R(y_R - y_R^0)\chi_{j'}^P(y_P - y_P^0)\Phi_{k'}(y_N), \tag{4.63}$$

where x is electronic coordinate, y's are nuclear coordinates with y_N standing for the "bridge" (linker) mode. $\chi's$ are used for local vibrational wave functions and $\Phi's$ are used for bridge mode vibrational states. The vibrations of the bridge are included in the rate calculations through the interaction Hamiltonian which couples electronic states Ψ_P, Ψ_R of reactants and products. In the Fock representation, it takes the form:

$$H^{\text{int}} = \sum_N \beta^0 e^{-\alpha y_N}(a_N^+ a_{N+1} + a_{N+1}^+ a_N), \tag{4.64}$$

where β^0 is the exchange interaction energy of the orbitals N and $N+1$ at separation y_N^0. The bridge fluctuations enter the formula for the rate by a matrix element

$$\langle \Phi_k(y_N) | \exp(-\alpha y_N) | \Phi_{k'}(y_N) \rangle, \tag{4.65}$$

which modulates the overall donor-acceptor interactions. When only one local mode and one bridge mode are considered, the rate Eq. (4.61) yields:

$$k_{NA} = \frac{2\pi}{\hbar} |H_{if}^0|^2 \sum_k B(k,T) \sum_{i,i'} B(i,T) \langle k | e^{-2\alpha y_N} | k \rangle |\langle i | i' \rangle|^2 \delta((i-i')\hbar\Omega - \Delta E), \tag{4.66}$$

where i labels the local mode χ, k the bridge mode Φ and H_{if}^0 stands for the matrix element $\langle \Psi_I | H^{\text{int}} | \Psi_F \rangle$. The bridge contribution to this rate can be easily calculated in the harmonic approximation of the bridge potential:

$$\langle \exp(-2\alpha y_N) \rangle = \exp\left(\alpha^2 \frac{\hbar}{m_{\text{eff}}\omega} \coth \frac{\hbar\omega}{2k_B T}\right). \tag{4.67}$$

Derivation of expectation value Eq. (4.67) follows standard analysis of a quantum oscillator in thermodynamic equilibrium. Average Eq. (4.67) is taken with the density operator for a harmonic approximation of the bridge modes y_N. The high temperature limit of this result is isomorphic with the derivation for a Brownian-motion model of time variations in the bridge coordinate [14]. It has been argued [99, 9] that fluctuations of the interatomic distances in covalently bridged donor-acceptor systems are insignificant and are not expected to have a strong effect on the transfer rate. In the extreme cases of high or low temperatures, bridge effects on the rate can be shown [102] to reduce to one effective oscillator with the frequency of a single vibration. The latter is quite large for typical bonds, (highest energy vibrational excitations corresponding to localized stretching modes of C=O or C-O bonds are in the range of 1500–2000 cm^{-1}, [87, 27, 10]), leaving the temperature effects irrelevant. For a covalent bond mediated tunneling pathway atomic vibrations are of very small amplitudes [99] and approximating the bridge as a rigid structure is an acceptable assumption. On the other hand, fluctuations of space distances $y_i(t)$ between intermediary molecules or residues across nonbonded gaps from their equilibrium values are expected to be relatively large, which would suggest a stronger dependence of the tunnelling matrix elements Eq. (4.60) on fluctuations in separation of interacting nonbonded groups. Generalization of Eq. (4.60) for these cases would include an explicit average of the Eq. (4.65)[21]

$$k_{NA} = \frac{2\pi}{\hbar}|H_{if}^0|^2 \prod_{i=1}^{N_S} \langle \exp(-2\alpha y_i)\rangle (FC)\,. \tag{4.68}$$

Time dependent variations in $y_i(t)$ can be described as a stochastic process. If the dynamic fluctuations in $y_i(t)$ have much shorter relaxation time scale

[21] Note that Eq. (4.66) represents a semiclassical approximation and gives the rate which is an average over the bridge coordinate configurations. Given a configuration of all slow coordinates frozen at some particular value, one can calculate the relevant correlation function for all the fast dynamics and derive expression for the rate at the fixed configuration. The final result should be averaged over the appropriate Boltzman distribution of configurations. In a purely quantum nonadiabatic ET process, the times of relevance are proportional to $\hbar$. This time scale characterizes the time required by a molecule near the transition state to decide to form a product or to fall back to the reactants population. Rigorously corrected rate constant for the system can be obtained as long as the motion along slow coordinates are slower than the "decision" process (to undergo reaction or to relax within the reactans well) but faster than the reaction itself. The observed rate is then the rate averaged over these fluctuations.

than $1/k$, the average in Eq. (4.68) can be taken over a stationary distribution function of the stochastic process $\{y_i(t)\}$ (provided the process is stationary and such a distribution exists [64, 47]). As an example, let us assume that the dynamics of a particular bridge mode $y(t)$ follows a standard overdamped Brownian motion. The average of the attenuation factor (*cf.* Eq. (4.68)) taken with the stationary probability distribution function $p_{\rm st}(y)$ for that process yields:

$$\langle \exp(-2\alpha y) \rangle = \exp(\alpha^2/\mu) = \exp(2\alpha^2 \langle (\delta y)^2 \rangle) \,, \tag{4.69}$$

where

$$\mu = \tfrac{1}{2} \langle (\delta y)^2 \rangle^{-1} \,, \tag{4.70}$$

and

$$\langle (\delta y)^2 \rangle = \beta m_{\rm eff} \omega^2 \,. \tag{4.71}$$

This result can be compared with the high-temperature limit of Eq. (4.68) which brings the same expression.

Analytical derivation of Eq. (4.61) with fluctuations imposed on y can be easily extended to a non-Gaussian diffusion governing the evolution of $\{y(t)\}$. Let us consider a model in which spatial fluctuations in the distance y are the sum of independent contributions of variations in cartesian coordinates $\{x_1, x_2, x_3\}$. The latter specify positions of intervening spacers mediating the transport through the protein. We assume that y has some "privileged" value which is equivalent to the position of a global minimum of a potential function in this coordinate (note that in a final definition of the $\{y(t)\}$ process, we impose a restoring force which "pushes" y towards its stationary average). Such a model illustrates breathing modes of globular proteins which tend to preserve their functional shape. Spatial variations in either of the directions x_1, x_2, x_3 are further assumed to be described by independent[22] Brownian motions, each characterized by a standard deviation σ^2 and some constant displacement per unit time, f. The process can be viewed as a (continuous in time and in space) limit of superposition of "random walks", (see [64]) in each cartesian coordinate, separately.

By repeated use of the Ito transformation formula (*cf.* Appendix A), one can show that the process $y(t)$ is a stochastic diffusion with the "position dependent" infinitesimal displacement and variance given by:

$$\phi(y) = \frac{\sigma_{x_i}^2}{y} - ry \,, \tag{4.72}$$

$$\sigma^2(y) = \sigma_{x_i}^2 = \sigma^2 \,, \tag{4.73}$$

[22] Let us note, that in general dynamic properties of different through space jumps $y_i(t)$ do not need to be statistically independent. In such a case, noise correlation effect will strongly influence characteristics of coherence in the system at hand [103].

where r stands for the spring coefficient of the restoring force proportional to the distance from the equilibrium value of y:

$$y = \sqrt{x_1^2 + x_2^2 + x_3^2} \tag{4.74}$$

and, for simplicity, we have assumed $f = 0$. The stationary probability distribution function $p_{st}(y)$ can be calculated directly by use of the FPE and it reads:

$$p_{st}(y) = \frac{4r^{3/2}}{\sigma^3\sqrt{\pi}} y^2 \exp(-ry^2/\sigma^2)\,. \tag{4.75}$$

Evaluation of the average Eq. (4.61) with the distribution function Eq. (4.75) yields:

$$\langle e^{-2\alpha y}\rangle = \left(\frac{2\alpha^2\sigma^2}{r} + 1\right) e^{\frac{\alpha^2\sigma^2}{r}} \left[1 - erf\left(\frac{\alpha\sigma}{\sqrt{r}}\right)\right] - \frac{2\alpha\sigma}{\sqrt{\pi r}}\,. \tag{4.76}$$

The above analysis can be generalized to cases which incorporate anharmonicity in the force field acting on y, as well as to situations where the coupling between the y-modes and thermal bath is nonlinear, leading to the position ("distance")-dependent infinitesimal diffusion coefficient $\sigma^2(y)$.

Suppose that the electron donor and acceptor are imbedded inside a protein. In such a molecule many bonds can rotate, bend or vibrate leading to large fluctuations in an interchromophore distance. Random variations of the latter can be described by a stochastic variable obeying *e.g.* a diffusive dynamics like the one described above.

The proper temperature dependent distribution of distance between contacts can be determined from the molecular dynamics calculations [9, 27, 11, 87]. From experiments [102, 96, 52] comes a rough estimation of α values (1.0 - 1.7 Å^{-1}) for typical exponential decay of ET rate in biological macromolecules (*cf. e.g.* models of ET from Zn-porphyrin group in *cytochrome c* to a ruthenium atom bond to a histidine residue, [25, 99, 100]). By assuming a mean square displacement $\langle(\delta y)^2\rangle$ to be of order of 1.0 Å^2, harmonic approximation in distance fluctuations (Eqs. (4.69), (4.70), (4.71)) yields the rate enhancement by a factor of 300 ($P = \langle e^{-2\alpha y}\rangle \approx 324$); a mean square displacement lower by one order of magnitute produces only a twofold enhancement of the rate ($P \approx 2.4$). A radial approximation to the potential (*cf.* formulae (4.72), (4.73), (4.74)) with the same parametrization for the dynamic effects estimation leads to $P \approx 0.98$ for $\alpha = 1.7\text{Å}^{-1}$, $\langle(\delta y)^2\rangle \approx 1\text{Å}^2$ and $P \approx 0.84$ for $\alpha = 1.7\text{Å}^{-1}$, $\langle(\delta y)^2\rangle^{1/2} \approx 0.15\text{Å}$, *i.e.* slightly "reduces" the rate.

A possible realization of conformational changes in the intervening medium can be modelled by a bond rotational isomerization [104] which occurs

when there exists a permissive bond orientation favoring the ET process. Treating the bonds as identical and independent and allowing them to fluctuate between the "correct" and "incorrect", we can formulate a hypothetical model in which ET transfer depends on the number of correct bond orientations interconverting according to the scheme:

$$A \underset{\gamma_2}{\overset{\gamma_1}{\rightleftarrows}} B\,, \tag{4.77}$$

where γ_1, γ_2 stand for frequencies of interconvertions between a correct (A) and incorrect (B) orientations within the group of, say, N bonds. Sampling a proper bond in the collection of N independent ones follows a binomial distribution (N, p_i) with $p_i = i(1-\gamma_1)/N + \gamma_2(N-i)/N$, where i is a starting number of correct bonds. The population of A-type bonds (*i.e.* the number of "proper" bonds, X) evolves in time as a Markov chain process [90] governed by the transition probability P_{ij}:

$$P_{ij} = \mathrm{Prob}\,[X(t+1) = j | X(t) = i] = \binom{N}{j} p_i^j (1-p_i)^{N-j}\,. \tag{4.78}$$

A vast family of similar models have been used in genetic modelling [64], description of protein folding [1] and analysis of ion-channel gating [104] in biological membranes.

For sufficiently large N, the proportion of proper bonds (*i.e.* the ratio of the number of A-type bonds to the global number of bonds N, X/N) becomes a continuous function of time (changes in the proportion of proper versus incorrect bonds are assumed to occur slowly in time). The associated stochastic process describes then evolution of a concentration $Y = X/N$, the unit of time in Y corresponding to an epoch of N time units in the original X process. Let us assume that for large N, frequencies γ_1, γ_2 scale as $\gamma_1 = \tilde{\gamma}_1/N, \gamma_2 = \tilde{\gamma}_2/N$. For $N \to \infty$, the associated process converges to a diffusion process (*cf.* Appendix A) with a drift coefficient $\phi(y) = -\tilde{\gamma}_1 y + (1-y)\tilde{\gamma}_2$ and a variance coefficient $\sigma^2(y) = y(1-y)$ (note that at the level of the Smoluchowski equation description, this model leads to a position-dependent diffusion coefficient). For long times, an asymptotic, "non-Gaussian" stationary probability distribution function in y-variable exists and is given by:

$$p_{st} = \frac{\Gamma(2(\tilde{\gamma}_1 + \tilde{\gamma}_2))}{\Gamma(2\tilde{\gamma}_1)\Gamma(2\tilde{\gamma}_2)} y^{2\tilde{\gamma}_2 - 1}(1-y)^{2\tilde{\gamma}_1 - 1} \tag{4.79}$$

leading to the estimation of the P factor in terms of the confluent hipergeometric function:

$$P = \langle e^{-2\alpha y} \rangle = {}_1F_1(2\tilde{\gamma}_2, 2(\tilde{\gamma}_1 + \tilde{\gamma}_2); -2\alpha)\,. \tag{4.80}$$

The estimates of γ_1, γ_2 should come from molecular dynamics studies or from experiments. In equilibrium conditions, the ratio γ_2/γ_1 can be related to an energy bias favoring a particular "correct" state of the bonds:

$$\beta E = -\ln \frac{\gamma_2}{\gamma_1}. \tag{4.81}$$

The main conclusion which can be drawn from the model is that,

- in a semiclassical approximation of the ET rate, conformational fluctuations can be crucial in understanding attenuation (or enhancement) of the tunneling matrix element,
- the overall effect on the rate depends on the particular type of dynamics underlying the fluctuations of the through space distances (or bridge displacements).

Phenomenology used in this Section can be applied to realistic ET situations provided sets of dynamic parameters could be obtained from separate molecular dynamics studies on particular systems of interest. From the multiple-pathways models developed by Beratan, Onuchic *et al.* [10] comes information of inhomogeneous distribution of through bond and through space electronic coupling in a long-range macromolecular ET. All of the methods of calculating H_{if} described by the authors predict that due to distribution of chemical interactions, the protein is an inhomogeneous barrier to ET. As such, the electronic coupling is found to be sensitive to the structure of the intervening medium and the distance between the chromophores.

Our analysis focused on the cases where the molecular processes responsible for variations of the through space distances/ bridge displacements can be approximated by stationary stochastic processes evolving on time scales shorter than the ET transfer. Their equilibration has been assumed to be described by a stationary probability distribution function in the parameter describing the net distance between the chromophores.

As an example of ET process mediated by the proteic medium, let us briefly discuss the dynamics of the primary charge transfer in photosynthesis [105, 106]. According to molecular dynamics studies performed on the models of photosynthetic chromophores [11, 107, 88], the amplitude of the interchromophore distance fluctuations yields rms values of 0.15Å or less. Given these fluctuations are Gaussian in nature, formulae (4.69) yield estimation of electronic coupling enhancement, $P = 1.14$ which would suggest about 14% fluctuations in the kinetic rate. In fact, recent observations of relaxation in photosynthetic reaction centers bring evidence of nonexponential decay (*cf.* [86, 87] and reference therein).

Weakening the assumption of gaussianity (as in the model of a bond rotational izomerization) could significantly change the above result (the

conclusion can be infer from the shape of the stationary probability function, *cf.* Eq. (4.79)). The bell-like, approximately Gaussian shape of it can be obtained in the range of frequencies $\tilde{\gamma}_1 > 1/2, \tilde{\gamma}_2 > 1/2$. Otherwise, bond orientation acts as a gating mechanism for the transfer.

Our discussion of the electronic factor is based on semiclassical approximation which is valid if there is no phase coherence between the energy levels of the reaction coordinate. Derivation of formulae Eqs. (4.65), (4.68) requires assumption of the Born–Oppenheimer separation of all nuclear modes. In a transition between two states, there is a probability that multiple attempts at the transition will add coherently. Such a situation would correspond to a molecule passing through the transition state, having some amplitude to mix from reactants to products and then waiting for a complete oscillation of the reaction coordinate back to the transition state configuration. If the damping in the reaction coordinate is sufficiently low, it is possible for the molecule to return to the transition state with a "memory" of the phase of the wave function on the previous pass [108]. The vibrational coherence effect has recently been observed in the fs time resolved absorption spectra of photosynthetic reaction centers by Vos *et al.*, [105]. Together with observations of nonexponential relaxation in photosynthetic reaction centers, the findings have spurred speculations about the mechanism of the primary charge transfer in photosynthesis [83]. The underdamped vibrational motions with periods about 2 ps that seem to explain experimental observations of coherence have been also identified in molecular dynamics studies of Gehlen *et al.*, [87]. It has been concluded, however, that they are of little consequence to the ET process, as they are weakly correlated with fluctuations in vertical energy gap determining kinetics of the transfer. Rather, in according to the models presented here and in agreement with findings of Marchi *et al.* [11], motions affecting H_{if} must be responsible for the nonexponential relaxation. The issue of quantum coherence in ET processes could be addressed by exact quantum dynamical calculations based on spectral densities produced in molecular dynamics (MD) calculations.

Relaxing the assumption of an adiabatic elimination of molecular motion in the dynamics (*i.e.* in the net distance between the chromophores) used in the above analysis would require evaluation of the kinetic rate by direct incorporation of the fluctuation-correlation time which would go beyond a standard golden-rule approximation [37, 108].

4.5. ET in the primary steps of photosynthesis

The conversion of light energy to chemical energy during photosynthesis involves the transfer of electrons between pigments embedded in a membrane protein. Interest in the chemical physics of photosynthetic reaction centers (RC) has been spurred by X-ray crystallographic elucidation

of the structures of two such systems [109]. In the purple bacteria *Rps. viridis*, the RC is composed of two symmetrically related branches of pigments (chromophores), L and M, and proteic subunits which provide the necessary scaffolding to hold the chromophores in place (*cf.* Fig. 4.5). The pigment molecules include four bacteriochlorophylls (BChl), two bacteriophyophytins (BPh) and two quinnone molecules. Two branches of RC are joined by a *bacteriochlorophyll b* dimer, the so called special pair $(BChl)_2$.

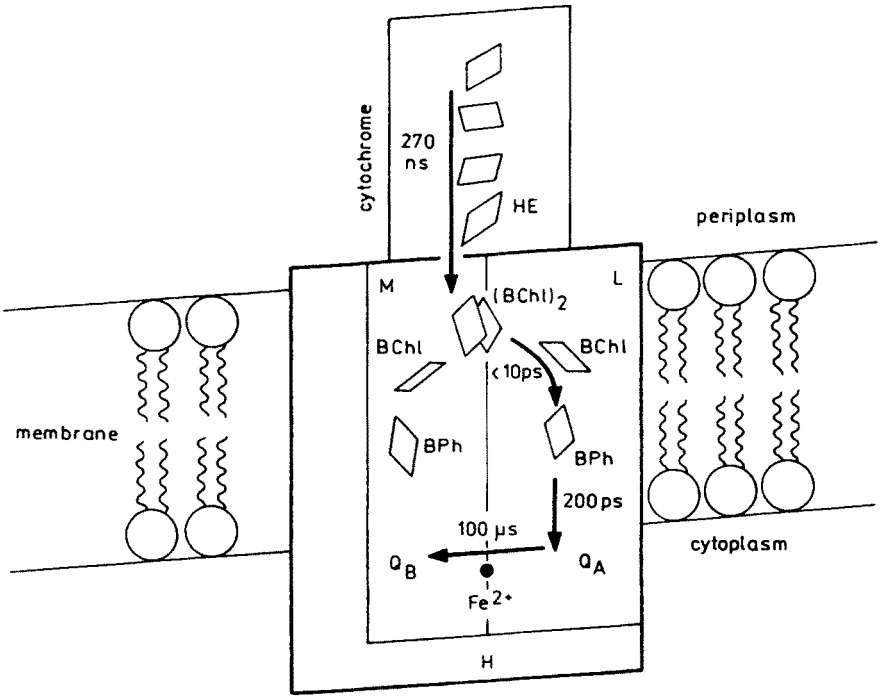

Fig. 4.5. Structural arrangement of the chromophores in the reaction center of *Rps. viridis* with the L, M, H and cytochrome protein subunits. The BChl and BPh abbreviations stand for the *bacteriochlorophyll b* and *bacteriopheophytin b*, *HE* for haeme groups, Q_A for menaquinone and Q_B for ubiquinone. The electron transfer half-lifetimes (k_{ET}^{-1}) are averaged values from recently published experimental data [105, 106].

The primary charge separation is the process of the electron transfer from the photoexcited special pair to the bacteriopheophytin at the L side of the system. There are many remarkable aspects about the process. The quantum yield of ET is close to 100% and about 40% of the input photon

energy is stored in the transmembrane charge separation. Despite a large center-to-center distance $\sim$ 17Å, the observed ET rate is at least 10^3 times faster than the expected rate over that distance in a vacuum. The primary ET step, although far from being thermally activated, speeds up as the temperature is lowered from 300 to 10 K. The forward and backward rates differ by many orders of magnitude. Further, even with the near-C_2 symmetry of the RC, the reaction occurs only along the L branch. These features are the primary concern of the molecular modeling, theoretical and experimental efforts aimed at understanding photosynthetic electron and energy transfer.

Structural information alone is not enough for the analysis of the dynamic process in a complex system like the RC. In order to apply the theory of ET rates we need much more information on

- electronic couplings that depend on electronic states, intermolecular distances and intervening medium molecules
- averaged Franck–Condon factors that depend on the medium vibronic structure and fluctuations
- intramolecular vibronic properties
- medium relaxation.

Such information is only partially available. The best way to proceed is to use all available experimental information for the construction of the models along with the guidelines of the basic theory.

The photophysical properties of chlorophylls depend on the electronic configuration of their valence orbitals in the ground and excited states. Knowledge of these configurations is required for understanding of the ET dynamics. The wave functions and orbital energies of the various states are sensitively probed by spectroscopic methods (*cf.* [85, 86, 110, 17]). In order to properly analyze optical and high-resolution EPR and ENDOR spectra and derive information about electronic configurations, reliable quantum mechanical calculations are indispensable.

The fundamental theoretical approach for the electronic structure would be parameter-free *ab initio* quantum mechanical calculations of the wave functions and energies. This type of calculations are not, however, feasible for large biological systems. As an alternative one has rather to resort to semiempirical molecular orbital methods which rely on an adequate parametrization of specific interaction integrals defined by a specific Hamiltonian and pertinent many-electron functions (see Appendix B).

Recent structural data for porphyrins and their derivatives, the bacteriochlorophylls (*cf.* Fig. 4.6) have demonstrated the skeletal flexibility of chromophores [111, 19, 83]. Experimental redox and optical results for puckered porphyrins have also established that such conformational variations can affect the highest occupied (HOMO) and the lowest unoccupied

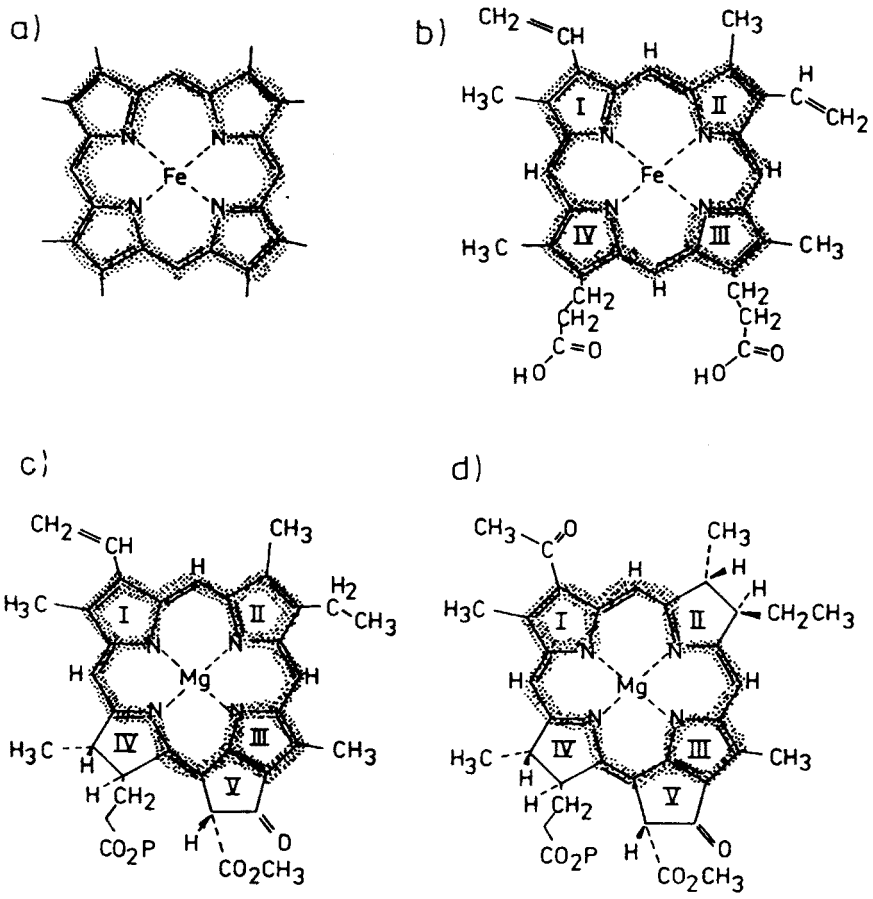

Fig. 4.6. Comparison of a porphyrin (a) a protoheme (b) with a chlorophyll (c) and a bacteriochlorophyll (d). The π system of each macrocycle composed of conjugated carbons has been shown as the shaded areas. Molecular x and y axes are defined by positions of nitrogens of rings II and IV (X-axis) and the nitrogens of rings I and III (Y-axis).

(LUMO) molecular orbitals of the chromophores and thereby modulate their light absorption properties.

This concept has been applied by the author [17] to study models of photosynthetic chromophores with the aim to delineate the factors controlling their electronic properties. The calculations on models of bacteriochlorophyll molecules (BChl) and on original crystallographic structures, employed the "spectroscopic INDO" method (*cf.* Appendix B) de-

veloped by Zerner and coworkers [112]. Ground electronic states were obtained as closed-shell molecular orbital (MO) wavefunctions in the Restricted Hartree–Fock (RHF) framework. Low-lying excited states whose energies are available from spectroscopic data [88, 83] were approximated by configuration interactions (CI) among configurations generated as single excitations from the RHF ground state.

It is helpful in this context to consider the 4-orbital model of Gouterman [110], Fig. 4.7 which focuses attention on the two highest-lying MO's (HOMO, HOMO+1) and the two lowest-lying unoccupied MO's (LUMO, LUMO-1). Gouterman has shown that single excitations involving these four orbitals provide a good CI basis for approximating low-lying Q-bands of porphyrins in visible and near-infrared region.

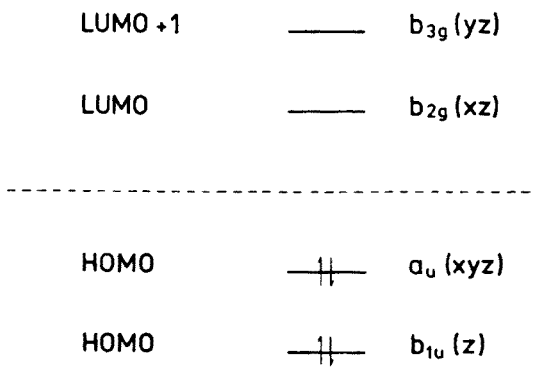

Fig. 4.7. Schematic representation of the molecule orbitals involved in the four-orbital model of porphyrins. The indicated orbitals refer to the D_{2h} subgroup appropriate to the idealized conjugated framework of the BCL molecule (pyrrole rings I and III are bi sected by the yz plane and rings II and IV by the xz plane. The transformation properties of the four orbitals are indicated in parentheses by appropriate functions of cartesian coordinates.

While the crystallographic coordinates of natural BChl molecules dealt with have no rigorous symmetry elements, it is useful for schematic purposes to assume an idealized D_{2h} symmetry for the conjugated BChl framework (see Fig. 4.6) and accordingly, the four orbitals are assigned to the appropriate irreducible representations in the D_{2h} subgroup of D_{4h}. In D_{2h} symmetry, the HOMO is the a_u orbital and the lower of the unoccupied b_{2g}, b_{3g} pair is the b_{2g} orbital. The dominant contributions to the lowest excited state are expected to be $a_u \rightarrow b_{2g}$ with some contribution from $b_{1u} \rightarrow b_{3g}$. Since these configurations can only be coupled to the ground state by y-polarized light under electric dipole selection rules, the transi-

tion to this state is designated Q_y. The other two excitations arising in the model are expected to provide the major contributions to the Q_x transition.

In the ZINDO calculations all single excitations involving the highest 15 occupied and the lowest 15 unoccupied MO's were included as a reference level to test the four-orbital model. Analysis of the calculated CI coefficients has revealed that $> 90\%$ of the Q_y excited state is accounted for by the HOMO→LUMO excitation. Much of the remainder is provided by the HOMO−1→LUMO +1 excitation, and the individual contributions from the other 223 excitations included in the CI calculations are all $< 1\%$. Since the Q_y transition is so dominated by a single configuration, it is not surprising that a good linear correlation (regression coefficient of 0.99) is obtained between the total excitation energy and the difference in HOMO and LUMO eigenvalues (even though the excitation energy is a many-electron quantity). Analysis of the HOMO and LUMO atomic orbital coefficients[23] shows that, in general, the pattern of π-orbital phases for a given nearest-neighbor pair of conjugated atoms is the same for each of several different conformational variants of BChls observed in the antenna protein complex of *Prosthecochloris aestuarii* (*cf.* [17] and references therein). The bonding or antibonding nature of the AO interaction in the HOMO and LUMO is generally independent of the particular BChl. The primary exception to this rule arises in the case of $C - N$ bonds in rings I and III, where the signs of the excited state bond-order contributions from the HOMO and LUMO vary among the different BChls structures, suggesting that the Q_y transition is especially sensitive to conformational deformations associated with these bonds.

Despite the lack of rigorous symmetry, calculated transition dipole directions deviated by less than 5° from the y-axis passing through the nitrogens of rings I and III, and the change in state dipole moment upon excitation[24] is found always to be along y-axis to within 10° of accuracy. Conformational effects on the spectra have been studied by use of the bare skeleton model, where all side substituents have been replaced by hydrogen

---

[23] We have focused on the π-type AOs of the conjugated atoms, taken as p_z orbitals, antisymmetric in the x, y plane containing the four nitrogen atoms (*cf.* Fig. 4.6).

[24] The calculated excited state is not strictly orthogonal to the ground state determined variationally in SCF calculations. That leads to an extra overestimation of electrostatic effects in INDO method. We have corrected calculations of the excited state dipole by using orthogonalized excited state orbital $|\Psi_f\rangle = (|\Phi\rangle - a|\Psi_g\rangle)/(1-a^2)^{1/2}$. In the last expression, a stands for the mixing between final(excited) and initial(ground) states.

atoms. Distortions from planarity of the conjugated macrocycle have been found to be a source of about 50 nm shift towards the red portion of the spectra.

The influence of substituents has been further analyzed by removing axial ligands and checking calculated spectral sensitivity to changing orientation of the side groups. We have found by ZINDO calculations that rotation of ring I acetyl group from an in-plane to an out-of plane configuration (*i.e.* the acetyl group is taken out of conjugation with the π-system of the porphyrin) leads to a blue shift of 680 cm^{-1} in the calculated spectra. This result, supported by experimental evidence [17] and references therein) can thus partially explain distribution of excited states observed in natural reaction centers [83, 88].

To help assess the possible role of the surrounding protein medium in influencing the Q_y excitation energies of the BChl subunits in *P. aestuarii* complex, we have carried out additional calculations. The amino-acids can affect the BChls through a number of mechanisms, including both long-range (involving induced and permanent multipole contributions) and short-range interactions. Amino-acids with aromatic groups [25] might be especially effective in modulating Q_y transition energies. Since several amino-acids are found in the immediate vicinity of one of BChls in *P. aestuarii* complex, we carried out calculations on structural models of the chromophore extended so as to include all aromatic residues containing atoms within the distance of 5.5 Åfrom the center of the chromophore[26]. No significant rotation of the transition dipole was observed, and the overall blue shift of $\sim$ 1150 cm^{-1} could be attributed almost entirely (80%) to the nearby positive charge associated with the charged group of the arginine residue. Focusing, therefore on amino acids with charged moieties on their side chains, we then carried out calculations for all chromophores, including such amino acids by using suitable point charges obtained from ZINDO calculations for the separate residues [27]. Our results show that the charged amino acid side chains can cause shifts in Q_y energy transitions[28] of as much as 2000 cm^{-1}, *i.e.* at least as large as the effect of acetyl group orientations and comparable in mag-

---

[25] Presence of such groups with delocalized π type orbitals gives rise to additional interactions within the π system of chromophores.

[26] Electrostatic effects have been found to be of negligible amplitude beyond that limit, *cf.* [17].

[27] The charged residues are negatively charged aspartic and glutamic acids and positively charged bases, histidine, arginine and lysine.

[28] The shifts can be either towards red or blue regon of the spectral lines, depending on the sign and location of the residue charges relative to the ground- and excited-state dipole moments of the BChls.

nitude to the overall spread of transition energies exhibited by the isolated chromophore molecules.

We shall note that the calculated environmental and electrochromic shifts should be interpreted as upper limits, since the calculated differences in ground- and excited-state dipole moments appear to be systematically exaggerated[29].

To sum up, theoretical calculations on structural data of natural chromophores indicate that axial ligands, hydrogen bonds and neighboring residues from the proteic media help to define a scaffolding that in turn controls the conformations of the molecules. ZINDO calculations on individual conformationally distinct, bacteriochlorophylls and chlorophylls predict different optical and redox properties that reflect crystallographically observed conformational variations among the molecules. The evidence of macrocycle distortions which are consonant with crystallographic results comes also from series of experimental ESR and NMR data [111, 85, 86, 19]. To estimate costs of conformational variations, we have performed ZINDO calculations on several synthetic porphyrins (*cf.* Fig. 4.6) in which different peripheral substituents were added in order to deliberately introduce steric crowding [19]. Best examples of this approach were severely saddle-shaped Zn(II) tetraphenyl-octaethyl (ZnTPOEP) and NiTPOEP porphyrins. ZINDO calculations predict that the puckered molecules are easier to oxidize wheras reduction is fairly insensitive to distortions[30]. As the temperature raises, fluctuations of the skeleton cause the different resonances to coalesce, yielding a free energy of activation for the inversion (or "flattening") of the macrocycle. We have further performed MD studies of the molecule by using a modified CHARMM force field [113, 75, 80, 19]. The calculated energy difference between the puckered and planar relaxed configurations yield 20.6 kcal mol^{-1}, the value to be compared with a difference of 9.8 kcal mol^{-1} between the most puckered and planar BChls in the antenna system of *Prosthecochloris aestuarii*, [19]. Relaxing of chromophores from their crystallographic positions towards planarity shrinks that energy to 1.7 kcal mol^{-1}.

In conclusion, our analysis suggests that protein micro-environment defines structural scaffolding and determines available conformations of molecules. Site-directed mutations may alter then the protein pocket and indirectly affect properties of natural chromophores whose optical and redox properties are responsible for directionality and rate of ET in natural biomolecules.

From quantum mechanical calculations we are able to estimate the electron-transfer integral H_{if} for various pairs of chromophores and pre-

[29] Numerically estimated change in state dipole for excited- versus ground-state ranges from 2 to $10D$ wheras experimental estimate is less than $3D$.

dict relative contributions of environmental factors to the donor-acceptor coupling intensity. MO numerical analysis allows also to assign values of partial electrostatic charges and their distribution in the complex before and after ET process. In a particular case of photosynthetic systems, quantum mechanical models of porphyrins and their derivatives give a better understanding of the principles of the harvesting of solar energy and its high yield conversion into final biochemical products. MO calculations are part of the project to design synthethic systems that mimic the efficiency and selectivity of the biological reaction. This step of theoretical modelling is a hallmark for further molecular dynamics studies which aim to evaluate the strength and relaxation properties of state-energy fluctuations in the ET systems.

Theoretical evaluation of the rate constants requires some assumptions on the range of parameters involved in the description of ET process (*cf.* Eqs. (2.8), (2.17)). The existing information sources are experimental data, MO calculations, MD simulations and phenomenological models of kinetics in complex systems based on *e.g.* the theory of stochastic processes. The latest allow to incorporate the nonequilibrium effects of fluctuating medium polarization and set up conditions for adiabatic/non-adiabatic ET process. A full description of the ET rate at the level of biological systems is, however, a formidable task and remains an area of active theoretical development.

5. Summary

Theoretical problem of quantitatively understanding electron transfer processes in complex aperiodic macromolecular structures such as proteins remains a fascinating technical and scientific challenge, for which we have tried in this overview to outline the available tools and methods. For theoreticians who probe the control of quantum electronic tunneling in proteins and the interplay of classically treated nuclear degrees of freedom, there is still a long way to go. One of crucial arguments to be resolved in biological ET is whether the protein acts as an inhomogeneous or homogeneous electronic coupling medium. This question can be addressed by theoretical calculations of parameters involved in the kinetics: the transfer integral H_{if} which couples donor-acceptor states, energetics of initial and final states, their sensitivity to structural perturbations. An important goal is to combine complementary methods stemming from a statistical theory of rate processes with quantum mechanical estimates of ET dynamics in complex polar medium.

Our theoretical calculations on structural models of photosynthetic ET systems strongly suggest (Section 4.5) that conformational variations observed for porphyrin derivatives can provide a mechanism for altering optical

and redox properties. Such effects, in combination with additional modulations induced by protein residues (or solvents) (Section 4.4 an d 4.5), thus provide an attractive mechanism for fine-tuning the electronic properties of the chromophores *in vitro* and *in vivo*. By constructing phenomenological models of ET transport in natural reaction centers (Sections 4.2, 4.3, 4.4) we have shown occurrence of nonexponential kinetics observed in the systems (*cf.* (4.40), (4.41), 4.53) and pointed out possible sources of "non-standard" (non-Arrhenius) temperature and free energy dependence of ET reactions (*cf.* Eqs. (4.37), (4.38)). We have discussed also shortcomings of the phenomenological approach based on the use of the theory of a dissipative two-level system (Sections 2.2 and 4.2). Nonadiabatic kinetic rate derivation for such systems lose their reliability when, due to system inhomogeneity, the characteristic relaxation time of the solvent becomes enhanced changing the degree of "nonadiabaticity" of the reaction (*cf.* Eqs. (2.17), (4.37), (4.38)). An exciting challenge in the field is to determine what qualitative differences might arise in the ET rates as protein secondary and tertiary structure vary along with donor-acceptor redox potentials and inter-chromophore distances. To answer those questions, large-scale molecular dynamics calculations are needed with reliable sets of electronic structures energies estimated from prior quantum mechanical calculations. Future work should address also dynamical issues of the medium whose relaxation properties can overlap with the inherent time of the ET. We believe that further investigations of biologically relevant but structurally simpler systems could help to discriminate among various models of ET in proteic media.

The study of biomolecules has been an important contribution to the physics of complexity. We hope, that within the scope of this review we were able to provide the reader with some insights into the protein "paradigm" for complex systems with a diversity of connections between structure, dynamics and functionality.

This paper is a compendium of a series of papers written at the Brookhaven National Laboratory and at the Université Pierre et Marie Curie, Paris. Thanks to a fruitful collaboration with Jack Fajer and Marshall D. Newton I have been introduced to enigmas of electron transfer processes in natural systems. Michel Moreau, Bernard Gaveau and Daniel Borgis are kindly acknowledged for sharing their enthusiasm and interest in defining kinetic rates in stochastic medium. My special gratitude is devoted to Prof. Andrzej Fuliński for his constant help and encouragement throughout this work.

Appendix A

Ito transformation formula

A continuous time parameter Markovian process, for which the sample paths $\{x(t)\}$ are continuous functions of time, is called a diffusion process. The stochastic diffusion process is fully determined by two moments:

$$\lim_{h\to 0}\frac{1}{h} < \Delta_h X(t)|X(t)=x >= \phi(x,t)\,, \tag{A.1}$$

$$\lim_{h\to 0}\frac{1}{h} < \{\Delta_h X(t)\}^2|X(t)=x >= \sigma^2(x,t)\,, \tag{A.2}$$

where $x\in\Omega$, $\Delta_h = X(t+h)-X(t)$. The functions $\phi(x,t)$ and $\sigma^2(x,t)$ are called expected infinitesimal displacement (drift coefficient) and infinitesimal variance, respectively. In addition to infinitesimal relations (A.1), (A.2) higher order infinitesimal moments are zero. Based on (A.1) and (A.2), it can be shown [90] that the probability density function for the process follows the evolution equation:

$$-\frac{\partial P(x,t'|y,t)}{\partial t} = \phi(x,t')\frac{\partial P(x,t'|y,t)}{\partial x} + \frac{1}{2}\sigma^2(x,t')\frac{\partial^2 P(x,t'|y,t)}{\partial x^2}\,. \tag{A.3}$$

A continuous, strictly monotonic function g with continuous derivatives g' and g'' may be used to transform an arbitrary stochastic diffusion process $\{X(t)\}$ into another diffusion process $\{Y(t)\}$, $y=g(x)$ by use of so called Ito transformation formula [90]. Infinitesimal parameters of the transformed process are:

$$\phi_Y(y) = \tfrac{1}{2}\sigma^2(x)g''(x) + \phi(x)g'(x)\,, \tag{A.4}$$

$$\sigma_Y^2 = \sigma^2(x)[g'(x)]^2\,. \tag{A.5}$$

Appendix B

Principles of INDO method

INDO (Intermediate Neglect of Differential Orbitals) is one of commonly used semiempirical molecular orbital (MO) methods. The Hamiltonian for the outer electrons in a molecule is written as

$$H = H_{\text{core}} + \sum_{i<j} r_{ij}^{-1} \tag{B.1}$$

using the Born–Oppenheimer approximation and neglecting spin-orbital, spin-spin and relativistic effects. H_{core} stands for the sum of the kinetic and potential energies of all outer (valence) electrons in the field of the core, and the double sum is the total energy of the Coulomb repulsion of all pairs of electrons i and j (the elementary charge e entering the Eq. (B.1) is set to 1 in atomic units). The full wavefunction of the system is approximated by using a finite linear combination of antisymmetrical functions of MO's Φ_{ki} (the index K labels a particular electronic configuration):

$$\Psi = \sum_{k}^{K} A_k \Phi_k(\Phi_{k1}, ..., \Phi_{kn}) , \tag{B.2}$$

and the coefficients A_k are determined by the application of variation principle to minimize the total energy

$$E = \frac{\langle \Psi | H | \Psi \rangle}{\langle \Psi | \Psi \rangle} . \tag{B.3}$$

The functions Φ_k are represented by determinants

$$\Phi_k = \det |\Phi_{k1}, ...\Phi_{kn}| \tag{B.4}$$

of MOs of electrons in different configurations. The number (K) and type (k) of configurations admitted in Eq. (B.2) determines the degree of configuration interaction (CI) considered. By limiting considerations to the closed shell systems, one can introduce an effective one-electron Fock operator F:

$$F\Phi_i = \varepsilon_i \Phi_i , \tag{B.5}$$

which is self consistently constructed by applying N atomic orbitals (AO) to build a molecular orbital

$$\Phi_i = \sum_{m}^{N} c_{im} \phi_m , \tag{B.6}$$

with the square of coefficients c_{im} representing the electron density in the atomic orbital ϕ_m in the molecular orbital Φ_i. In this formalism, the Fock matrix can be represented as

$$F_{\mu\nu} = h_{\mu\nu} + \sum_{\lambda,\sigma}^{N} P_{\lambda,\sigma} \left[(\mu\nu|\lambda\sigma) - \tfrac{1}{2}(\mu\lambda|\nu\sigma) \right] , \tag{B.7}$$

with $h_{\mu\nu}$ standing for the core integral

$$h_{\mu\nu} = \int \phi_\mu(1) H_{\text{core}} \phi_\nu(1) d\tau_1 \,, \tag{B.8}$$

$(\mu\nu|\lambda\sigma), (\mu\lambda|\nu\sigma)$ representing two-electron Coulomb integral and the exchange integral, respectively,

$$(\mu\nu|\lambda\sigma) = \int\int \phi_\mu(1)\phi_\nu(1) r_{12}^{-1} \phi_\lambda(2)\phi_\sigma(2) d\tau_1 d\tau_2 \,, \tag{B.9}$$

and $P_{\lambda\sigma}$ being the electron density matrix

$$P_{\lambda\sigma} = 2 \sum_{i=1}^{occ} c_{\lambda i}^* c_{\sigma i} \,. \tag{B.10}$$

The variation principle applied to a closed-shell system

$$\frac{\partial E}{\partial c_{\mu i}} = 0 \qquad \forall \mu, i \tag{B.11}$$

leads to the set of Roothaan–Hall equations:

$$\sum_{\nu=1}^{N} (F_{\mu\nu} - \varepsilon_i S_{\mu\nu}) c_{i\nu} = 0 \tag{B.12}$$

for the set of orbital energies ε_i and MO coefficients $c_{i\nu}$. The elements of the matrix $S_{\mu\nu}$ are the AO overlap integrals $\int \phi_\mu \phi_\nu d\tau$.

Equation (B.12) is solved iteratively until a self-consistency is reached. The final SCF solution [31] yields desired MOs Φ_i and their orbital energies ε_i. The ground state (B.4) electron configuration is produced by filling the orbitals with all electrons in the order of increasing energy.

The SCF calculations done with a set of M basis functions requires the computation of M^4 matrix elements. In order to make a treatment of large molecules possible, one has to reduce the complexity by either replacing the effect of inner core electron s by effective (pseudo-) potentials or by applying the semi-empirical SCF method which neglects most of the matrix elements $(\mu\nu|\lambda\sigma)$ and parametrize the remaining ones.

---

[31] Quantum chemistry distinguishes between the SCF equation, which hold for a finite basis set, and the Hartree–Fock limit, obtained when the asis set becomes complete.

The common MO methods differ mainly in: the type and number of AOs admitted to Eq. (3.5), the degree of neglect of the numerous two-electron Coulomb integrals in the Fock operator (Eqs. (B.7), (B.9)), the determination of the core integrals, the degree to which self-consistency of Eq. (B.12) is carried out and the t ype and number of electron configurations considered in Eq. (B.2). The zero-differential overlap approximation (ZDO) is the one which assumes a vanishing "differential" overlap

$$\phi_\mu \phi_\nu d\tau = 0 \tag{B.13}$$

between different AO basis functions in all points of space. In consequence, only two-electron integrals of the form

$$(\mu\mu|\nu\nu) = \gamma_{\mu\nu}\,, \tag{B.14}$$

involving only pairs of AOs have to be retained. The ZDO approximation requires a semiempirical treatment of short-distance behaviour of $\gamma_{\mu\nu}$ and of all diagonal and off-diagonal core integrals $h_{\mu\nu}$. The INDO method includes all valence orbitals. The term "intermediate neglect" points to the retention of one-center-two-electron exchange integrals $(\mu\nu|\mu\nu)$ (*cf.* Eq. (B.9)). Within the Zerner's version of INDO (ZINDO) approximation [112], basis orbitals ϕ_i are envisioned to be strongly orthogonal and

$$\begin{aligned}(\mu^A\nu^B|\lambda^C\sigma^D) &\equiv \delta_{AB}\delta_{CD}\int\int \phi_\mu^A(1)\phi_\nu^B(1)r_{12}^{-1}\phi_\lambda^C(2)\phi_\sigma^D(2)d\tau_1 d\tau_2 \\ &= (\mu^A\nu^A|\lambda^A\sigma^A) \qquad A = C \\ &= (\mu^A\nu^A|\lambda^C\sigma^C) \qquad A \neq C\,,\end{aligned} \tag{B.15}$$

where ϕ_μ^A is the atomic orbital centered on atom A. In order to maintain rotational invariance, two-center integrals ($A \neq C$) are evaluated over atomic orbitals $\tilde{\phi}_\mu^A$ that are s symmetric but have the same exponents and expansion coefficients as ϕ_μ^A. Equation (B.15) also suggests that all one-center integrals are maintained in this approach.

The main difference between ZINDO (designed to deal with optical spectra of porphyrin derivatives) and INDO is a modified parametrization of one center core integrals $h_{\mu\mu}$ and "resonance integrals" (*i.e.* the two-center terms $h_{\mu\nu}$, commonly called $\beta_{\mu\nu}$ integrals). The resonance integrals are taken proportional to the AO overlap $S_{\mu\nu}$:

$$\beta_{\mu\nu} = \beta_{AB} S_{\mu\nu}\,, \tag{B.16}$$

where β_{AB} depends only on the chemical nature of the atoms A and B carrying the AOs ϕ_μ, ϕ_ν. In ZINDO method the one-center core integrals

$h_{\mu\mu}$ are obtained from ionization potentials and the resonance integrals are purely empirical parameters set to reproduce experimental spectra.

The ground state SCF calculations reported in the text (Section 4.5) have been followed by a configuration interaction (CI) of lowest single-excited configurations between some number of HOMOs and LUMOs. All calculations have been calibrated by calculating Q_y transition energies for analogues of BChls, whose spectra are available from experimental data. The single Bchl model contained about 100 atoms, 240 basis functions and 200 valence electrons. The coordinates of heavy atoms utilized crystallographic data of chromophores obtained from the Brookhaven Protein Data Bank. Hydrogens were placed at standard distances and checked to ensure that no unacceptable steric interactions were generated.

All calculations were performed on a local Sun-Sparc station and on the Cray Y-MP located at Florida State University, Tallahassee, USA.

REFERENCES

[1] D.L. Stein, *Spin Glasses and Biology*, World Scientific, Singapore 1992.

[2] L. Peliti, ed. *Biologically Inspired Physics*, NATO Advanced Research Workshop, 1989, Plenum Press, New York 1990.

[3] S. Glasstone, K.J. Laidler, H. Eyring, *The Theory of Rate Processes*, McGraw-Hill, New York 1946.

[4] C.A. Macken, A.S. Perelson, *Proc. Natl. Acad. Sci. USA* **86**, 6191 (1989).

[5] J.D. Bryngelson, P.G. Wolynes, *J. Phys. Chem.* **93**, 6902 (1989).

[6] I.E.T. Iben, D. Braunstein, W. Doster, H. Freuenfelder, *Phys. Rev. Lett.* **62**, 1916 (1989).

[7] J. Klafter, M.F. Schlesinger, *Proc. Natl. Acad. Sci. USA* **87**, 848 (1986).

[8] R. Zwanzig, *Proc. Natl. Acad. Sci. USA* **85**, 2029 (1988).

[9] A. Kuki, *Electronic Tunneling Pathways in Proteins*, in *Structure and Bonding* **75**, Springer-Verlag, Berlin 1991.

[10] D.N. Beratan, J.N. Onuchic, J.J. Hopfield, *J. Chem. Phys.* **86**, 4488 (1987).

[11] M. Marchi, J.N. Gehlen, D. Chandler, M. Newton, *J. Am. Chem. Soc.* **115**, 4178 (1993).

[12] J.N Onuchic, P.G. Wolynes, *J. Phys. Chem.* **92**, 6495 (1988).

[13] E. Gudowska–Nowak, *J. Phys. Chem.* **98**, 5257 (1994).

[14] E. Gudowska–Nowak, *Neural Network World*, **4**, 151 (1995).

[15] B. Gaveau, E. Gudowska–Nowak, R. Kapral, M. Moreau, *Phys. Rev.* **A46**, 825 (1992).

[16] M. Moreau, D. Borgis, B. Gaveau, J.T. Hynes, R. Kapral, E. Gudowska–Nowak, *Acta Phys. Pol.* **B23**, 367 (1992).

[17] E. Gudowska–Nowak, M.D. Newton, J. Fajer, *J. Phys. Chem.* **94**, 5795 (1990).

[18] E. Gudowska–Nowak, *Acta Phys. Pol.* **B25**, 1161 (1994).

[19] J. Fajer, K. Barkigia, K. Smith, E. Zhong, E. Gudowska-Nowak, M. Newton, *Micro-Environmental Effects on Photosynthetic Chromophores* in *Structure and Function of Bacterial Reaction Centers*, ed. M.E. Michel-Beyerle, Springer-Verlag, Berlin 1991.
[20] R. Markus, *J. Chem. Phys.* **43**, 679 (1965).
[21] M.D. Newton, *Chem. Rev.* **91**, 767 (1991).
[22] T. Fonseca, *J. Chem. Phys.* **91**, 2869 (1989).
[23] R.A. Kuharski, J.S. Bader, D. Chandler, M. Sprik, M.L. Klein, R.W. Imprey, *J. Chem. Phys.* **89**, 3248 (1988).
[24] A.J. Leggett, S. Chakravarty, A.T. Dorsey, M.P. Fisher, A. Garg, W. Zwerger, *Rev. Mod. Phys.* **57**, 1 (1987).
[25] S. Larsson, *J. Chem. Soc. Faraday. Trans.* **79**, 1375 (1983).
[26] S. Larsson, M. Braga, A. Broo, B. Kaellebring, *Int. J. Quant. Chem.* **18**, 99 (1991).
[27] J.M. Gruschus, A. Kuki, *J. Phys. Chem.* **97**, 558 (1993).
[28] P. Wolynes, *J. Chem. Phys.* **86**, 3836 (1987).
[29] H. Frauenfelder, P.G. Wolynes, *Science* **229**, 337 (1985).
[30] R. Marcus, N. Sutin, *Biochim. Biophys. Acta* **811**, 265 (1985).
[31] M.D. Newton, N. Sutin, *Annu. Rev. Phys. Chem.* **35**, 437 (1984).
[32] A. Kuki, P. Wolynes, *Science* **236**, 1647 (1987).
[33] L.D. Zusman, *Chem. Phys.* **49**, 295 (1980).
[34] L.D. Zusman, *Chem. Phys.* **119**, 51 (1988).
[35] J.T. Hynes, *J. Phys. Chem.* **90**, 3701 (1986).
[36] E.A. Carter, J.T. Hynes, *J. Chem. Phys.* **93**, 2184 (1989).
[37] P. Haenggi, P. Talkner, M. Borkovec, *Rev. Mod. Phys.* **62**, 251 (1990).
[38] M.A. Thompson, M.C. Zerner, J. Fajer, *J. Phys. Chem.* **95**, 5693 (1991).
[39] L. Landau, *Sov. Phys.* **1**, 89 (1932).
[40] M. Redi, J.J. Hopfield, *J. Chem. Phys.* **72**, 6651 (1980).
[41] H.A. Kramers, *Physica* **7**, 284 (1940).
[42] K. Lindenberg, B.J. West, *The Nonequilibrium Statistical Mechanics of Open and Closed Systems*, VCH, Cambridge 1990.
[43] B.J. Gertner, K.R. Wilson, J.T. Hynes, *J. Chem. Phys.* **90**, 3537 (1989).
[44] R. Zwanzig, *Lect. Theor. Phys.* **3**, 106 (1961).
[45] H. Mori, *Prog. Theor. Phys.* **33**, 423 (1965).
[46] G. Tarjus, D. Kivelson, *Chem. Phys.* **152**, 153 (1991).
[47] N.G. Van Kampen, *Procesy stochastyczne w fizyce i chemii*, PIW, Warszawa 1990.
[48] R.F. Fox, *J. Stat. Phys.* **16**, 259 (1977).
[49] S. Okuyama, D.W. Oxtoby, *J. Chem. Phys.* **84**, 5824 (1986).
[50] P.G. Wolynes, *J. Chem. Phys.* **86**, 1957 (1987).
[51] P. Talkner, H.B. Braun, *J. Chem. Phys.* **88**, 7357 (1988).
[52] M.J. Weaver, *Chem. Rev.* **92**, 463 (1992).
[53] D.W. Dawidson, R.H. Cole, *J. Chem. Phys.* **19**, 1417 (1950).
[54] J. Jaeckle, C.A. Condat, *Phys. Rev.* **A39**, 2112 (1989).
[55] T.A. Vilgis, *J. Stat. Phys.* **1**, 47 (1987).

[56] R. Lefever, W. Horsthemke, *Noise Induced Transitions*, Springer Verlag, Berlin 1983.
[57] J. Masoliver, K. Lindenberg, B.J. West, *Phys. Rev.* **A34**, 1481 (1986).
[58] C. Van den Broeck, P. Haenggi, *Phys. Rev.* **A30**, 2730 (1986).
[59] D.L. Stein, R.G. Palmer, J.L. Van Hemmen, C.R. Doering, *Phys. Lett.* **A136**, 353 (1989).
[60] I. L'Heureux, R. Kapral, *J. Chem. Phys.* **88**, 7468 (1988).
[61] M.M. Dygas, B.J. Matkowsky, Z. Schuss, *SIAM J. Appl. Math.* **46**, 265 (1986).
[62] P. Haenggi, P. Riseborough, *Phys. Rev.* **A27**, 3379 (1983).
[63] I. L'Heureux, R. Kapral, *J. Chem. Phys.* **90**, 2453 (1989).
[64] N.S. Goel, N. Richter–Dyn, *Stochastic Processes in Biology*, Academic Press, New York 1974.
[65] G.H. Weiss, *Adv. Chem. Phys.* **13**, 1 (1967).
[66] S.H. Northrup, J.T. Hynes, *J. Chem. Phys.* **73**, 2700 (1980).
[67] R.F. Grote, J.T. Hynes, *J. Chem. Phys.* **73**, 2715 (1980).
[68] B. Hille, *Ionic Channels of Excitable Membranes*, Sinauer, Sunderland MA 1992.
[69] D. Colquhoun, A.G. Hawkes, *Proc. R. Soc. Lond. Biol.* **211**, 205 (1981).
[70] G.L. Millhauser, E. Salpeter, R.E. Oswald, *Proc. Natl. Acad. Sci. USA* **85** 1503 (1988).
[71] E. Jakobsson, S. Chiu, *Biophys. J.* **52**, 33 (1987).
[72] L. Liebovitch, T. Toth, *J. Theor. Biol.* **148**, 243 (1991).
[73] T.L. Croxton, *Biochem. Biophys. Acta* **946**, 19 (1988).
[74] D.G. Levitt, *Biophys. J.* **22**, 209 (1978).
[75] B. Roux, M. Karplus, *J. Am. Chem. Soc.* **115**, 3254 (1993).
[76] P. Lauger, *Biophys. J.* **53**, 877 (1988).
[77] V. Mannivannan, E. Gudowska–Nowak, R.T. Mathias, Description of cooperative channel gating, to be published in *Bull. Math. Biol.*, 1995.
[78] K. Manivannan, S.V. Ramanan, R.T. Mathias, P.R. Brink, *Biophys. J.* **61**, 216 (1992).
[79] S.V. Ramanan, P.R. Brink, *Biophys. J.* **65**, 1387 (1993).
[80] C.L. Brooks, M. Karplus, B.M. Pettit, *Proteins, a Theoretical Perspective of Dynamics, Structure and Thermodynamics*, Wiley Interscience, New York 1988.
[81] I.M. Klotz, *Arch. Biochem. Biophys.* **116**, 92 (1966).
[82] H. Frauenfelder, F. Parak, R.D. Young, *Annu. Rev. Biophys. Chem.* **17**, 451 (1988).
[83] R.A. Fleming, *Physics Today* **47**, 48 (1994).
[84] P.G. De Gennes, *J. Stat. Phys.* **12**, 463 (1975).
[85] C.K. Chan, T.J. DiMagno, X.Q. Chen, J.R. Norris, G.R. Fleming, *Proc. Natl. Acad. Sci. USA* **88**, 11202 (1991).
[86] Y. Jia, T.J. DiMagno, C.K. Chan, Z. Wang, M. Du, M. Schiffer, D.K. Hanson, J.R. Norris, G.R. Fleming, M.S. Popov, *J. Phys. Chem.* **97**, 13180 (1993).
[87] J.N. Gehlen, M. Marchi, D. Chandler, *Science* **263**, 499 (1994).
[88] A. Warshel, W.W. Parson, *Annu. Rev. Phys. Chem.* **42**, 279 (1991).

[89] E. Pollak, *J. Chem. Phys.* **93**, 1116, (1993).
[90] S. Karlin, H.M. Taylor, *A Second Course in Stochastic Processes*, Academic Press, New York 1981.
[91] C.R. Doering, J.C. Gadoua, *Phys. Rev. Lett.* **69**, 2318 (1992).
[92] A. Hodel, T. Simonson, R.O. Fox, A.T. Bruenger, *J. Phys. Chem.* **97**, 3409 (1993).
[93] P. Haenggi, *Chem. Phys.* **180**, 157 (1994).
[94] A.M. Stoneham, *Adv. Phys.* **28**, 457 (1979).
[95] A. Fuliński, *Phys. Lett.* **A180**, 94 (1993).
[96] G.L. Closs, J.R. Miller, *Science* **240**, 440 (1988).
[97] J. Tang, *J. Chem. Phys.* **98**, 6263 (1993).
[98] K. Mikkelsen, J. Ulstrup, M.G. Zakaraya, *J. Am. Chem. Soc.* **11**, 1315 (1989).
[99] J.J. Regan, S.M. Risner, D.N. Beratan, J.N. Onuchi, *J. Phys. Chem.* **97**, 13083 (1993).
[100] N. Sutin, B.S. Brunschwig, *Adv. Phys.* **226**, 65 (1990).
[101] H. Mc Connell, *J. Chem. Phys.* **35**, 508 (1961).
[102] T. Guarr, M.E. McGuire, G. Mc Lendon, *J. Am. Chem. Soc.* **107**, 5104 (1985).
[103] A. Fuliński, P.F. Góra, *Phys. Rev.* **E48**, 3510 (1993).
[104] M.B. Jackson, *J. Chem. Phys.* **99**, 7253 (1993).
[105] M.H. Vos, J.C. Lambry, J.C. Robles, D.C. Youvan, J. Breton, J.L. Martin, *Proc. Natl. Acad. Sci. USA* **89**, 613 (1991).
[106] M.H. Vos, F. Rappaport, J.C. Lambry, J. Breton, J.L. Martin, *Nature*, **363**, 320 (1993).
[107] K. Schulten, M. Tesch, *Chem. Phys.* **158**, 421 (1991).
[108] J.M. Jean, R.A. Friesner, G.R. Fleming, *J. Chem. Phys.* **96**, 5827 (1992).
[109] J. Deisenhofer, H. Michel, *The EMBO Journal* **8**, 2149 (1989).
[110] M. Gouterman, *J. Mol. Spectrosc.* **6**, 138 (1961).
[111] K.M. Barkigia, L. Chantranupong, K.M. Smith, J. Fajer, *J. Am. Chem. Soc.* **110**, 7566 (1989).
[112] J. Ridley, M. Zerner, *Theor. Chim. Acta* **32**, 111 (1973).
[113] K. Kuczera, J.-C. Lambry, J.-L. Martin, M. Karplus, *Proc. Natl. Acad. Sci. USA* **90**, 5805 (1993).